DESY Summerstudent's Lecture 2005:

Solid State Detectors

Robert Klanner, University of Hamburg

Chapter 1: Introduction

1.1 Aim of Lecture

- Introduction to Solid State (Silicon) Detectors:
  - Basic principles
  - Different detector types
  - Examples for applications
  - Limitations

Solid state detectors: a rapidly evolving field → attempt to present also recent developments

1.2 Literature

G.Lutz, Semiconductor Detectors, Springer

Various articles in NIM-A, IEEE-NS, (some references given on slides)

1.3 Index

1. Introduction
2. Parameters characterising detectors
3. Basics of solid state detectors – interaction of radiation with matter
4. Detector types
5. Limitations – in particular radiation hardness

1.4 Examples for solid state detectors and physics results achieved

- solid state detectors as radiation detectors used since the 50ies
- rapid development has started around 1980 due to
  - transfer of Si micro-electronics technology to detector fabrication (J.Kemmer NIM 169(1980)449)
  - start of miniaturisation of electronics → high density readout possible
  - interest in particles with short ($c\tau$ ~ 100 μm) lifetimes – charm, beauty, τ-lepton

Silicon Microstrip Detectors

- first successful use in a high energy physics: experiment NA32@CERN:

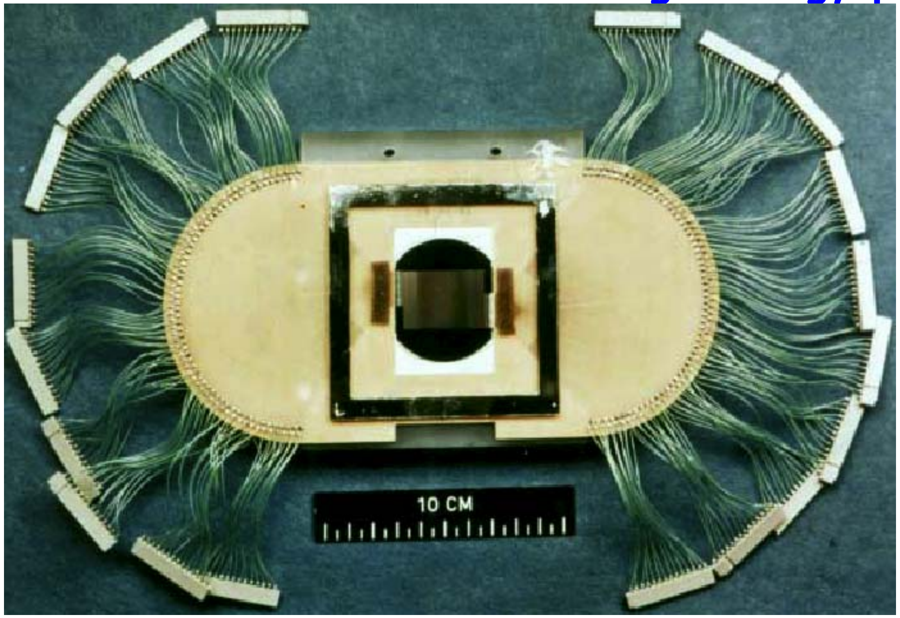

- 4μm resolution achieved
  ~1000 readout chs.

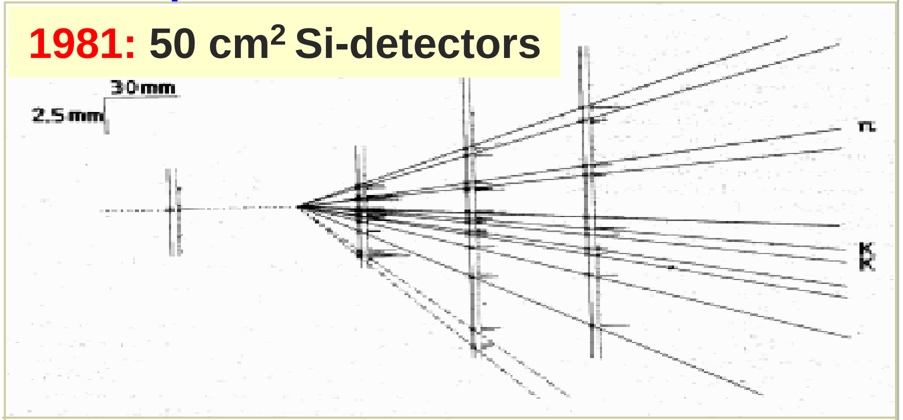

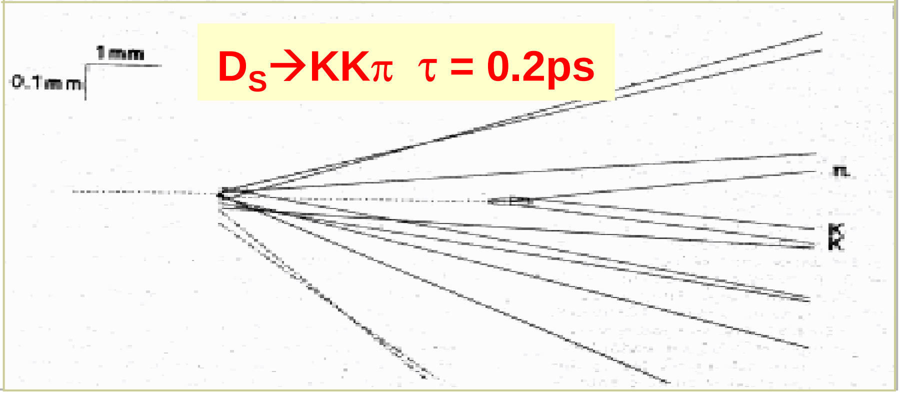

Silicon Strip Detector

essential for the discovery of the top-quark at FNAL (1994)
(and also LEP Higgs limit)

example:
CDF vertex detector

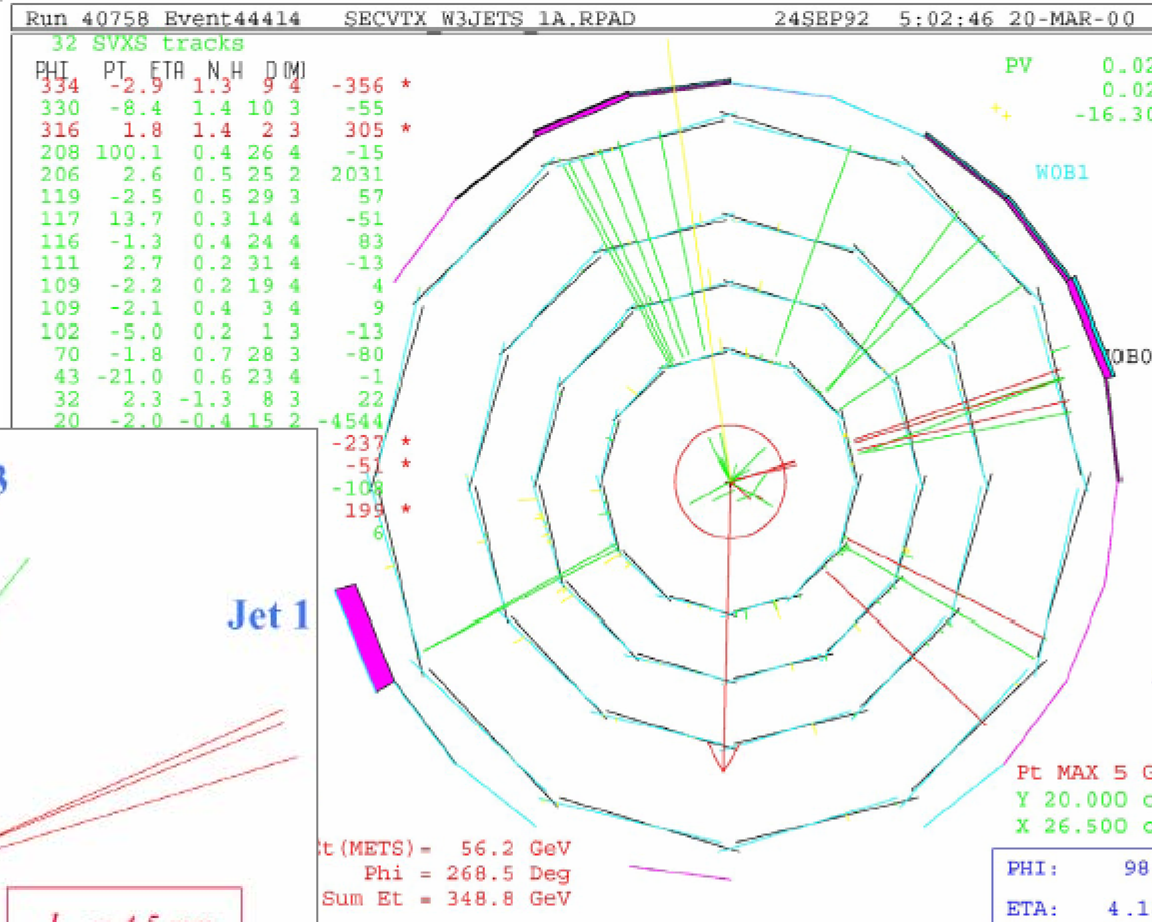

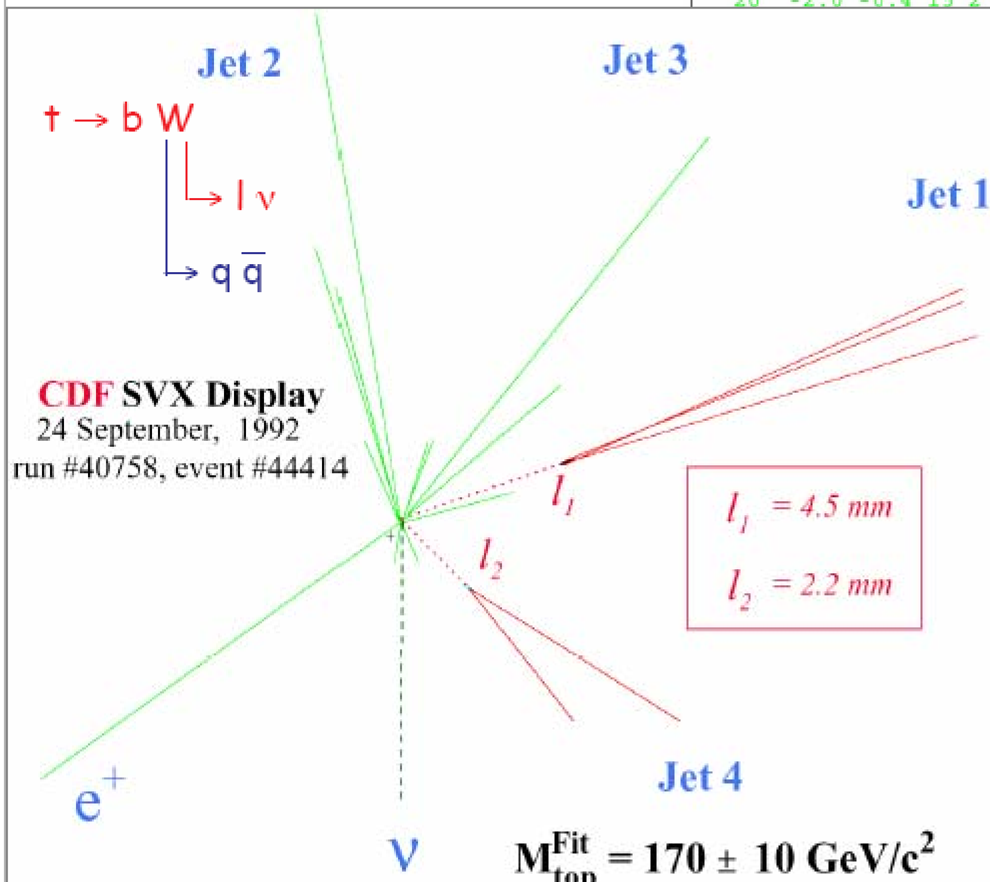

- **today:** CMS@LHC (CERN)
  ~200m2 and $9.65 \cdot 10^6$
  readout channels

Silicon Drift Detector invented in 1984 → one application low noise X-ray detection

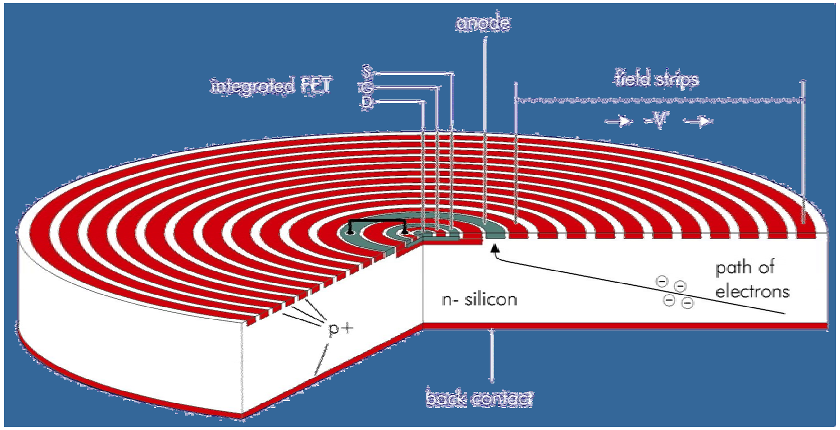

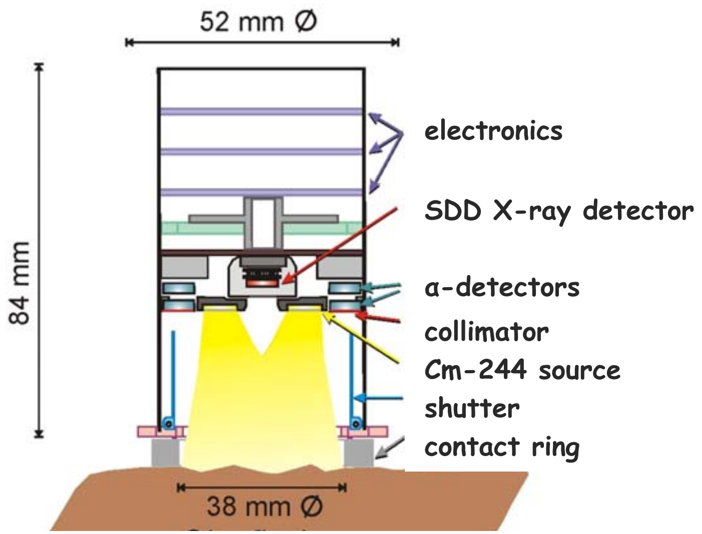

X-RAY SPECTRA OF MARS SOIL SAMPLES:

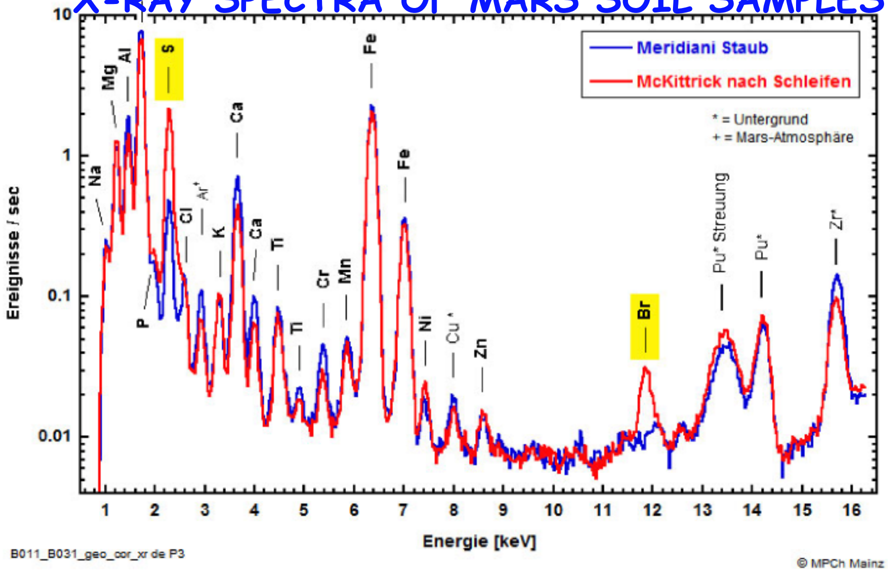

L. Strüder, IEEE-Nucl. Sci. Symposium (Rome 2004)
R. Rieder , MPI für Chemie, Mainz

Fully depleted CCD (based on drift chamber principle) – astronomy XXM-Newton

XMM-Newton satellite

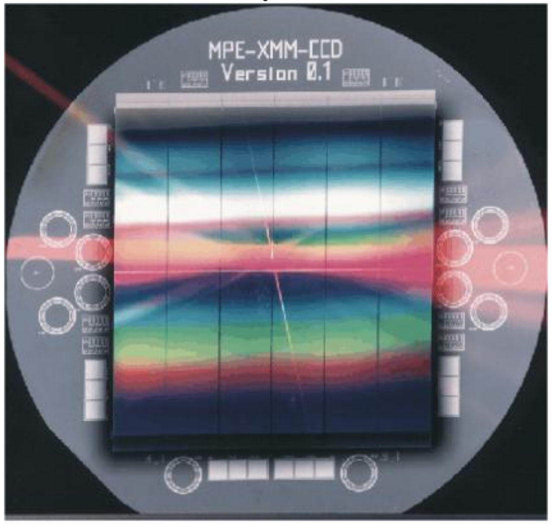

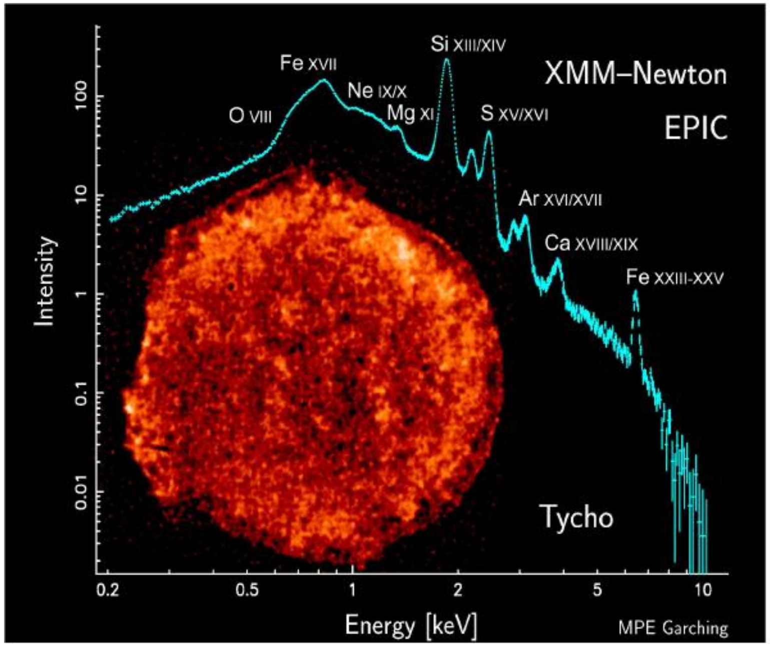

elemental analysis of TYCHO supernova remnant:

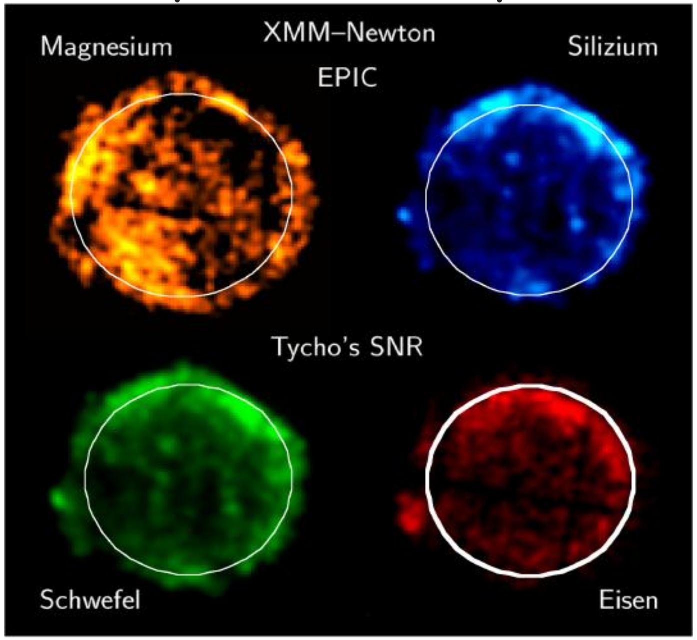

L. Strüder, IEEE-Nucl. Sci. Symposium (Rome 2004)

Controlled Drift Detector (CDD) for X-ray radiography

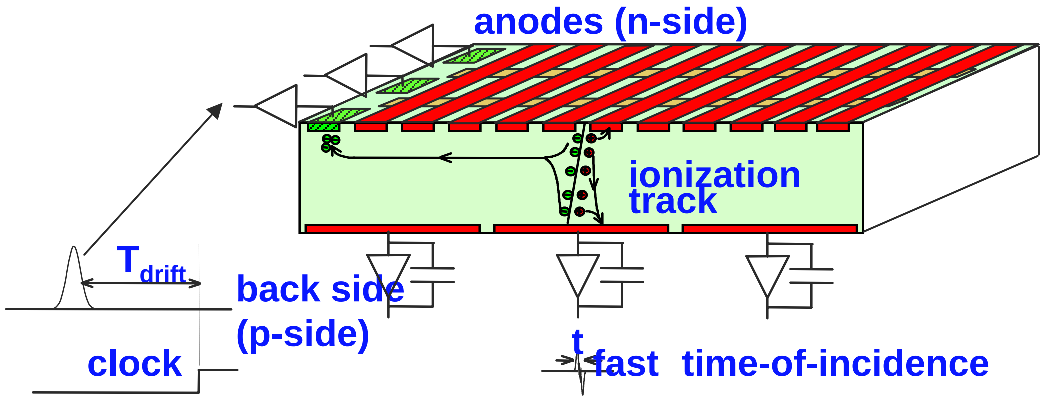

X-RAY RADIOGRAPHY:

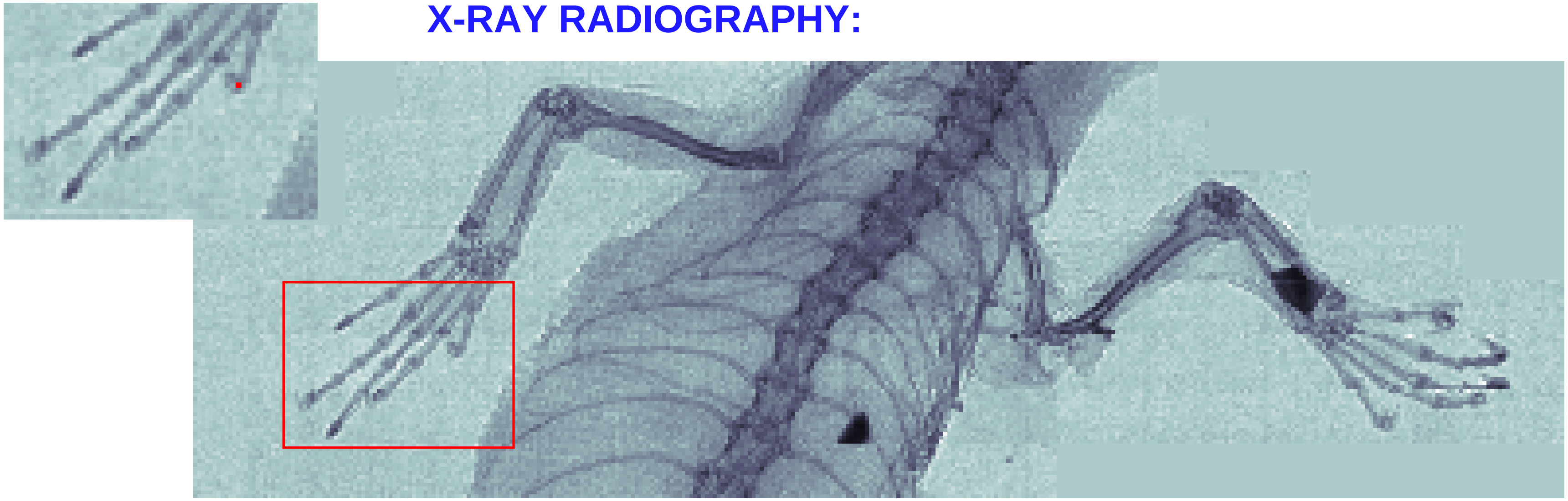

A. Castoldi et al, NIM-A518(2004)426

Chapter 2 – Parameters characterizing detectors

2.1 Introduction

(detector) ⊗ (readout) ⊗ (calibration) ⊗ (analysis) → all have to be understood !

Generic detector:

radiation/ particle → interaction energy deposit → signal light/charge → collect el.signal charge formation → el.signal processing → data recording →

→ calibration → analysis

Efficiency:

- **acceptance:** (recorded events)/(emitted by source): [geometry x efficiency]
- **efficiency/sensitivity**: (recorded events/particles passing detector)
- **peak efficiency**: (recorded events in acc.window/particles passing detector]

Response (resolution):

(spectrum from mono-) energetic radiation)

response to 661 keV γs

- Ge-detector
- organic scintillator

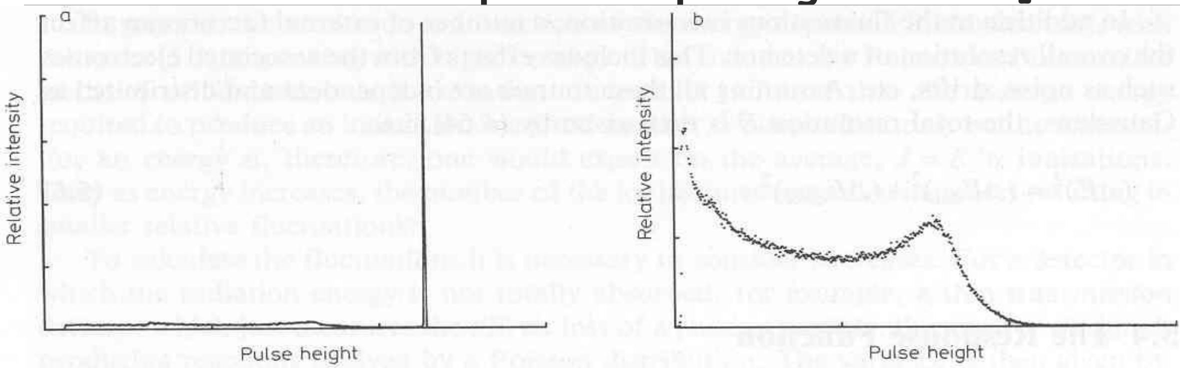

Fig. 5.2a, b. The response functions of two different detectors for 661 keV gamma rays. **(a)** shows the response of a germanium detector which has a large photoelectric cross section relative to the Compton scattering cross section at this energy. A large photopeak with a relatively small continuous Compton distribution is thus observed. **(b)** is the response of an organic scintillator detector. Since this material has a low atomic number Z, Compton scattering is predominant and only this distribution is seen in the response function

Reponse (resolution) continued:

- fact that response function is complicated is frequently ignored → wrong results !!

"good detector" aims for Gaussian response (with little non-Gaussian tails)

Calibration by N events with energy E

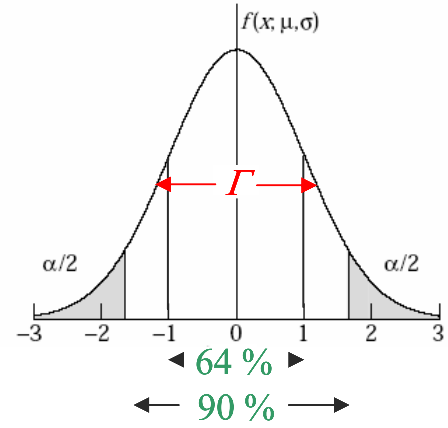

- mean: $$<S>=\frac{1}{N}\sum_i^N S_i, \quad \delta<S>=\sigma/\sqrt{N}$$
- rms resolution (σ): $$\sigma^2=\frac{1}{N-1}\sum_i^N (S_i-<S>)^2, \quad \delta(\sigma)=\sigma/\sqrt{2N}$$

for Gauss f.: (separate two peaks): $\Gamma=2\sqrt{2\ln 2}\,\sigma=2.355\sigma$

(for box with width a: $\sigma=a/\sqrt{12}$)

frequently <S> is not the best choice: e.g. Landau distribution: $\sigma\to\infty$

(median, truncated mean, are sometimes better choices !)

Calibration: $<S>=f(E)\cong c\times E+ped$

$$\sigma=g(E),\ \sigma/E\cong c_{calib}+c_{stat}/\sqrt{E}+c_{noise}/E\ \ (e.g.\ for\ energy\ measurement)$$

- c, ped … calibration constants depend on position, time (T,p,V,…)
- if c(E) … non-linear response

analogous for position-, time-, etc- measurements

Time response:

- **delay time:** time between particle passage (event) and signal formation
- **dead time:** minimum time distance that events can be recorded separately (depends on properties of detector and electronics ("integrating" or "dead") and on resolution criteria)
- **pile up effects:** overlapping events cause a degradation of performance
- **time resolution:** accuracy with which "event-time" can be measured

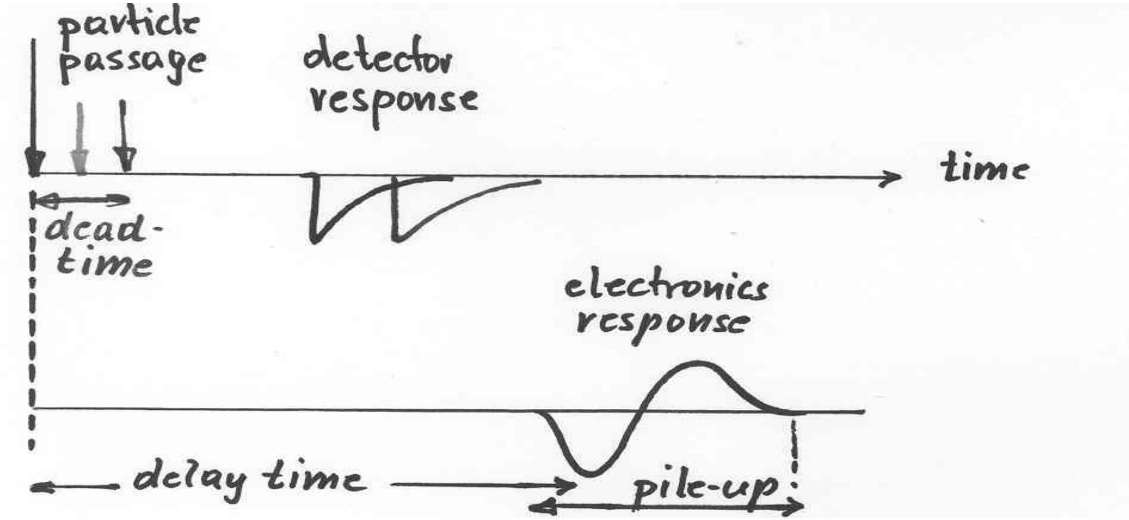

Example for counting losses due to dead time:

n… true interaction rate
m… recorded count rate
τ … system dead time

$$n = \frac{m}{1 - m \times \tau}$$

m$\times\tau$ is fraction time detector "dead" → rate at which true events lost: $n \times m \times \tau = n - m$
(for pulsed source – no effect if τ < 1/frequency)

Examples for pile-up effects:

612 LINEAR AND LOGIC PULSE FUNCTI

PULSE HEIGHT ANALYSIS SYSTEMS

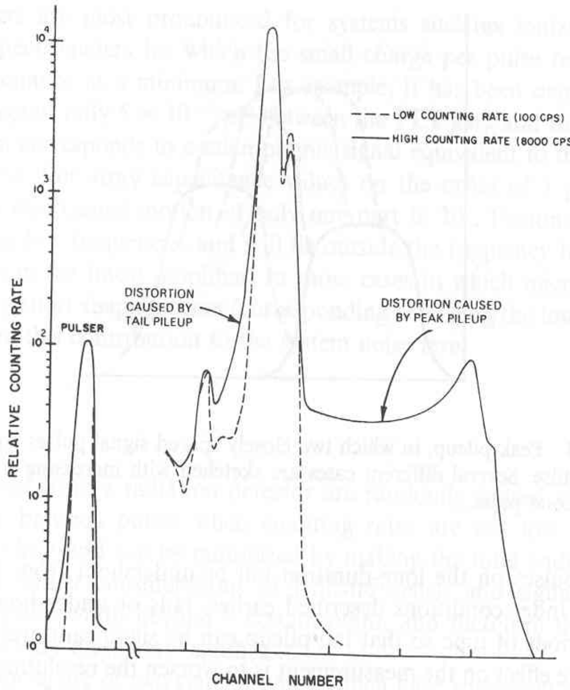

Figure 17-17 Spectral effects of peak and tail pileup. The dashed curve shows a ^{55}Fe spectrum taken at a low counting rate at which pileup is negligible. The solid curve shows a high-rate spectrum and illustrates the sum peak and continuum caused by peak pileup. The low-energy tail added to the primary peak by overshoot or tail pileup is also observed. (From Wielopolski and Gardner.[21])

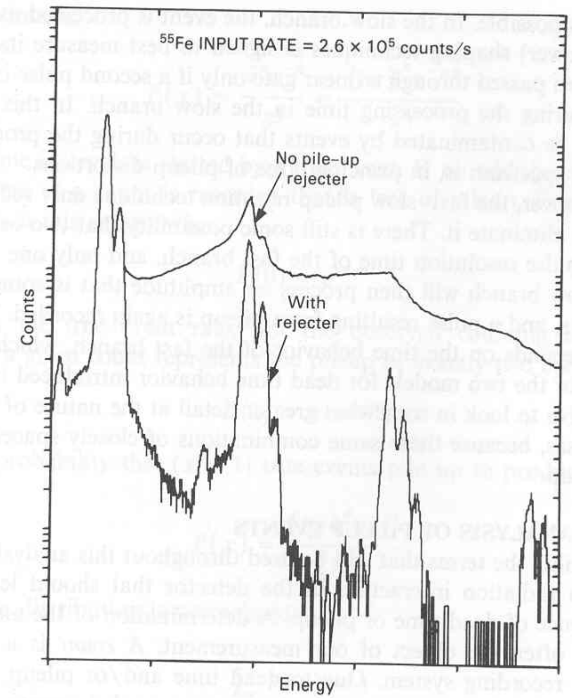

Figure 17-18 Pulse height spectra recorded with and without a pileup rejecter. The true event rate n was 2.6×10^5/s and the rejecter resolution time τ was 300 ns. Note that the contributions to the spectrum from pileup are greatly reduced by the rejecter, while the numbers of counts in the primary peaks (free of pileup) are unaffected. (From Goulding and Landis.[28])

→ distortion of spectra (loss in resolution) and overlapping events

→ situation can be optimized by "clever" electronics – requires understanding of pulse shape produced by detector !

2.2 Interaction of radiation with detector material

Property		Si	Ge	GaAs	Diamond
Atomic Number		14	32	31/33	6
Atomic Mass	[amu]	28.1	72.6	144.6	12.6
Band Gap	[eV]	1.12	0.66	1.42	5.5
Radiation Length X_0	[cm]	9.4	2.3	2.3	18.8
Average Energy for Creation of an Electron-Hole Pair	[eV]	3.6	2.9	4.1	~ 13
Average Energy Loss dE/dx	[MeV/cm]	3.9	7.5	7.7	3.8
Average Signal	[$e^-/\mu m$]	110	260	173	~ 50
Intrinsic Charge Carrier Concentration	[cm^{-3}]	$1.5 \cdot 10^{10}$	$2.4 \cdot 10^{13}$	$1.8 \cdot 10^{6}$	$< 10^{3}$
Electron Mobility	[cm^2/Vs]	1500	3900	8500	1800
Hole Mobility	[cm^2/Vs]	450	1900	400	1200

- **Solid State Detectors are ionization chambers**

- **energy required to "ionize" (produce one charge pair):**
  - ~30 eV for gases and liquids
  - 1-5 eV for solid state detectors
  - few meV to break up Cooper pairs (and to produce phonons)

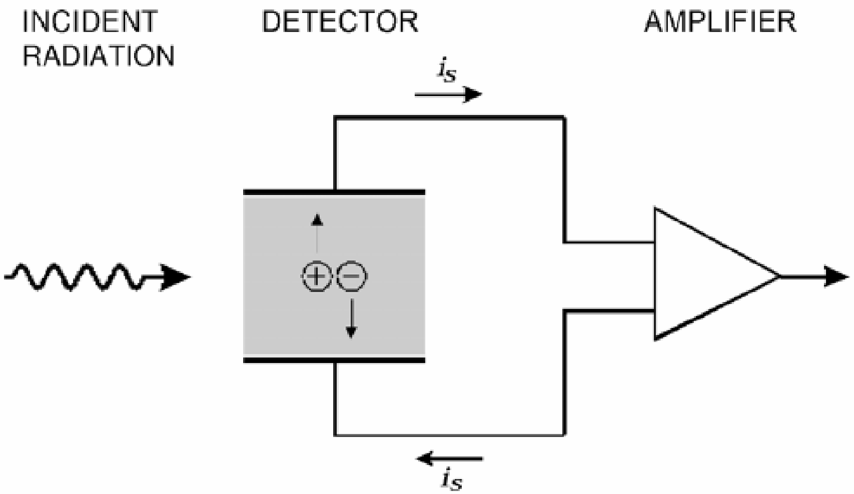

Detection of light

well suited for detection from the UV → IR

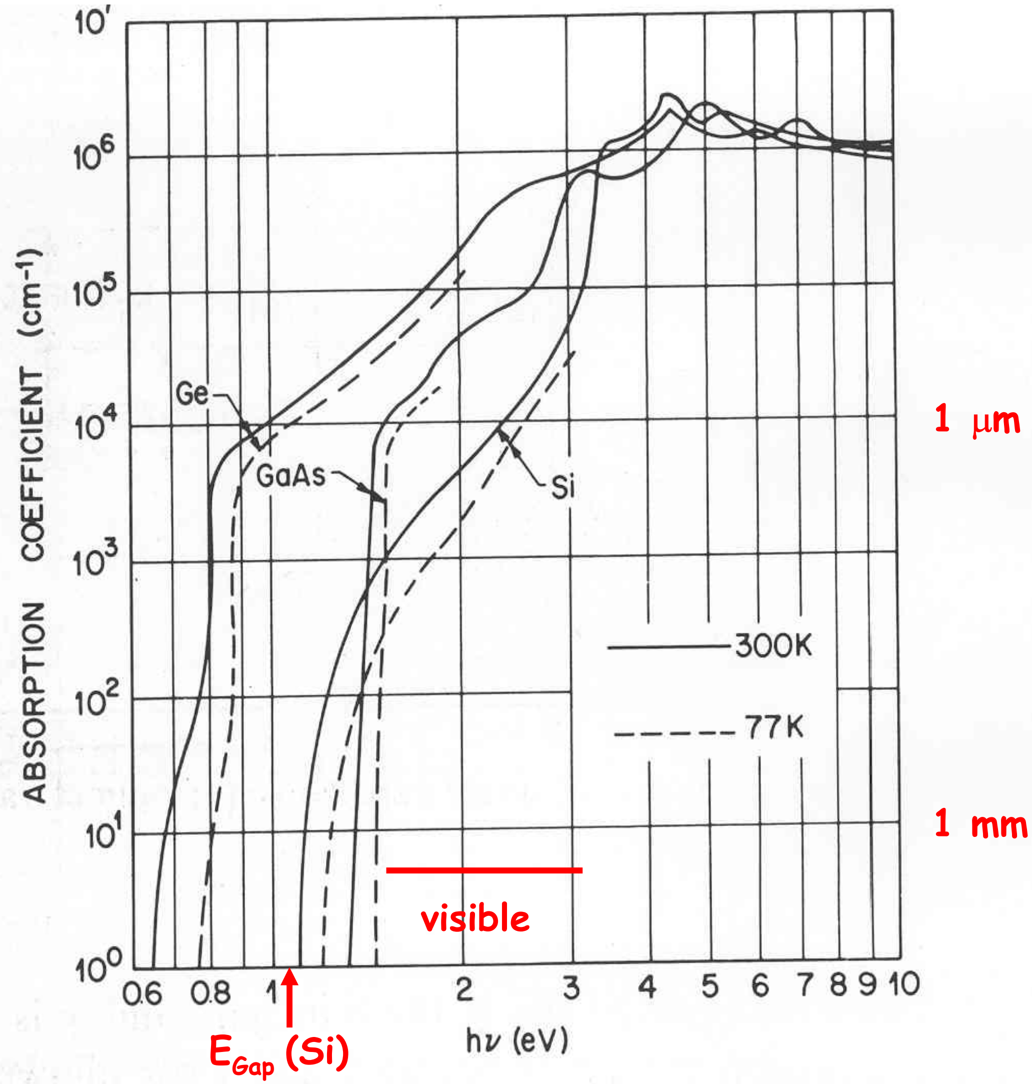

Fig. 27 Measured absorption coefficients near and above the fundamental absorption edge for pure Ge, Si, and GaAs. (After Dash and Newman, Ref. 51; Philipp and Taft, Ref. 52; Hill, Ref. 53; Casey, Sell, and Wecht, Ref. 54.)

Detection of charged particles:

(dE/dx = energy loss via Coulomb scattering off electrons - ionisation)

mean energy loss < dE/dx > - Bethe-Bloch formula vs β

from dE/dx(MIP):
Si: 110 (e-h)/μm
Ge: 260 (e-h)/μm

→ "healthy signal", which can be well processed by electronics

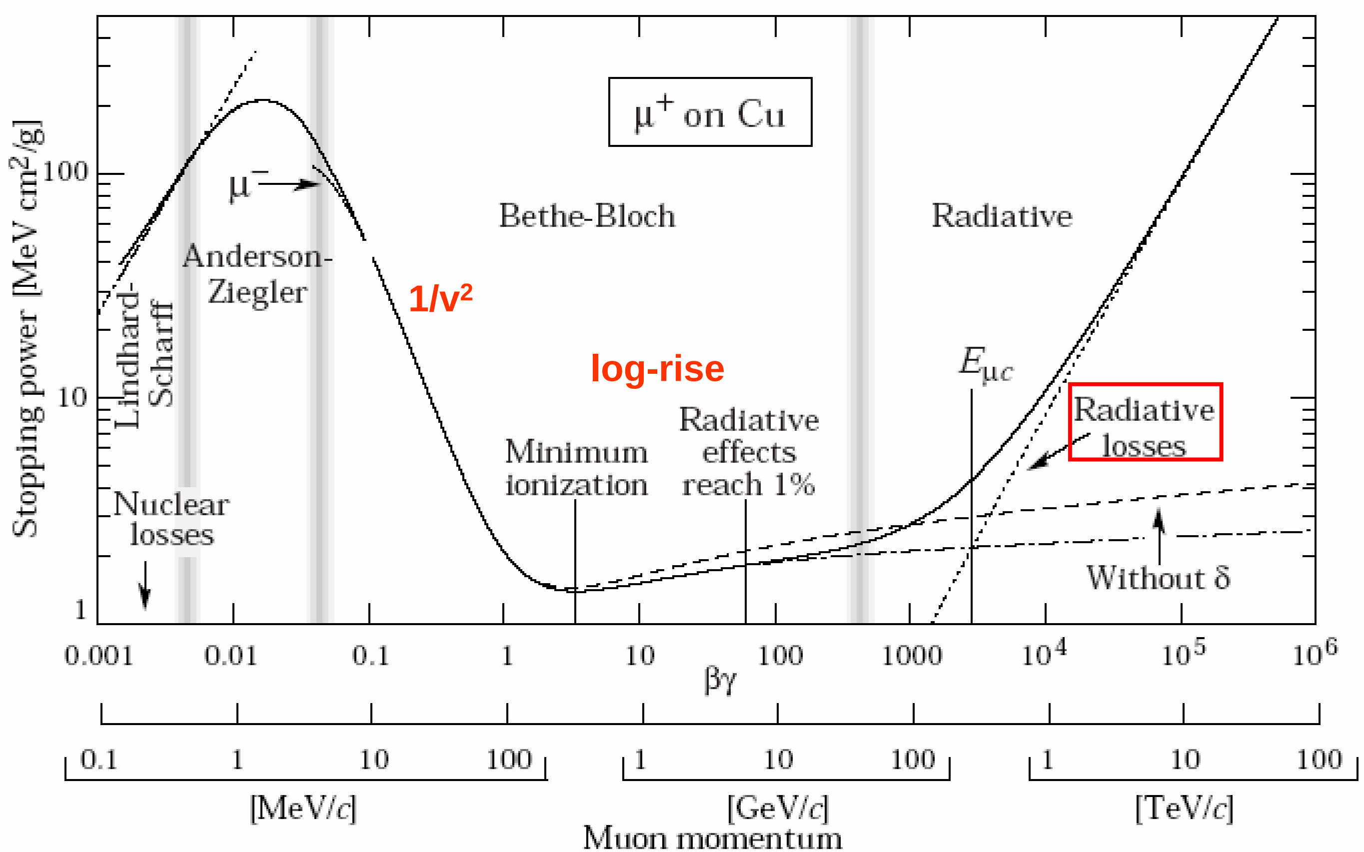

Fig. 27.1: Stopping power ($= \langle -dE/dx \rangle$) for positive muons in copper as a function of $\beta\gamma = p/Mc$ over nine orders of magnitude in momentum

Detection of charged particles: fluctuations in dE/dx-distribution

Bohr: simplified classical derivation of energy loss (stopping power) formula

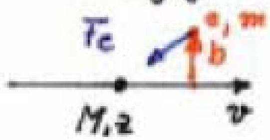

momentum transferred to electron:

$$\Delta\vec{p} = \int \vec{F}_E\, dt = e\int E_T\, dt = \frac{e}{v}\int E_T\, dx = \frac{2ze^2}{b\cdot v}$$

$$\left[\text{Gauss: } 4\pi z e = \int \vec{E}\, d\vec{\alpha} = 2\pi b \int E_T\, dx\right]$$

$\Rightarrow$ energy transferred: $\Delta E(b) = \frac{\Delta p^2}{2m} = \frac{2z^2e^4}{m v^2 b^2}$

for N_e (electron density) energy transferred for impact parameter interval $b, b+db$

$$-dE = \Delta E(b)\, N_e \cdot 2\pi b \cdot db \cdot dx \Rightarrow$$

$$-\frac{dE}{dx} = \left[\frac{4\pi z^2 e^4}{m\cdot v^2} N_e\right] \int_{b_{min}}^{b_{max}} \frac{db}{b} = [\ ]\cdot \ln\left(\frac{b_{max}}{b_{min}}\right)$$

b_{max} ... electrons bound $\Rightarrow \frac{b}{v} \lesssim \frac{1}{\nu}\gamma$

(ν... "orbital frequency electrons)

b_{min} ... energy conservation $\rightarrow T_{max}$

$$\rightarrow b_{min} \simeq \frac{ze^2}{\gamma m_e v^2}$$

$$\Rightarrow \boxed{\frac{dE}{dx} = \frac{4\pi z^2 e^4}{m v^2} N_e \ln\left(\frac{\gamma^2 m \cdot v^3}{z e^2 \nu}\right)}$$

contains essential features of Bethe Bloch, which has been derived using Quantum Mech.

energy distribution for electrons

distribution impact parameter:

$$dN = 2\pi b\, db$$

distribution of ΔE_e (in single collisions)

$$\frac{dN}{d(\Delta E)} = \frac{dN}{db}\cdot\frac{1}{d(\Delta E)/db} \propto 1/(\Delta E)^2$$

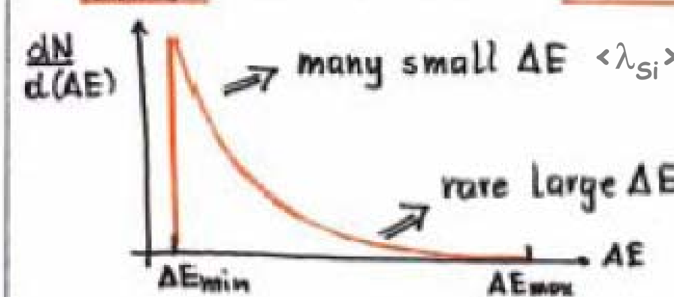

$\langle\lambda_{Si}\rangle = .25\mu m$

$\Rightarrow$ many collisions for material Δx

$$\boxed{\begin{array}{l}\text{large } \Delta E \rightarrow \text{high energy tail in distribution} \\ \rightarrow \delta\text{-(knock off) electrons) with finite range !}\end{array}}$$

Detection of charged particles: fluctuations in dE/dx-distribution

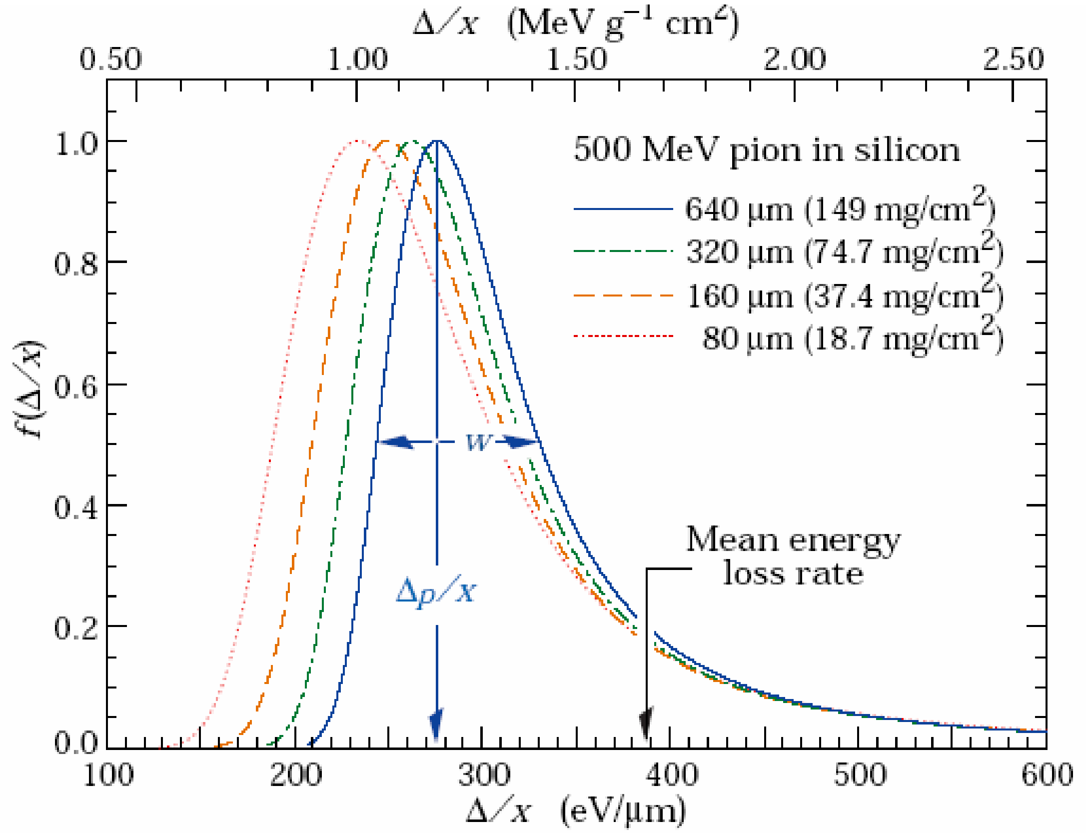

Figure 27.6: Straggling functions in silicon for 500 MeV pions, normalized to unity at the most probable value Δ_p/x. The width w is the full width at half maximum.

(H.Bichsel, Rev.Mod.Phys.60(1988)663)

→ shape of energy loss distribution depends on thickness of detector

(NB. for thin detectors < 1-2 μm finite probability of zero signal !)

Detection of charged particles: limitation of position accuracy

- most of ionisation in a narrow (< 1µm) tube around particle track,
- in addition few "high energy δ-electons" (high dE/dx-values) with finite range, which shift centre of gravity of deposited charge

→ "intrinsic" position accuracy degrades from O(< 1µm)

→ 10µm for dE/dx ~2xmop (most probable value)

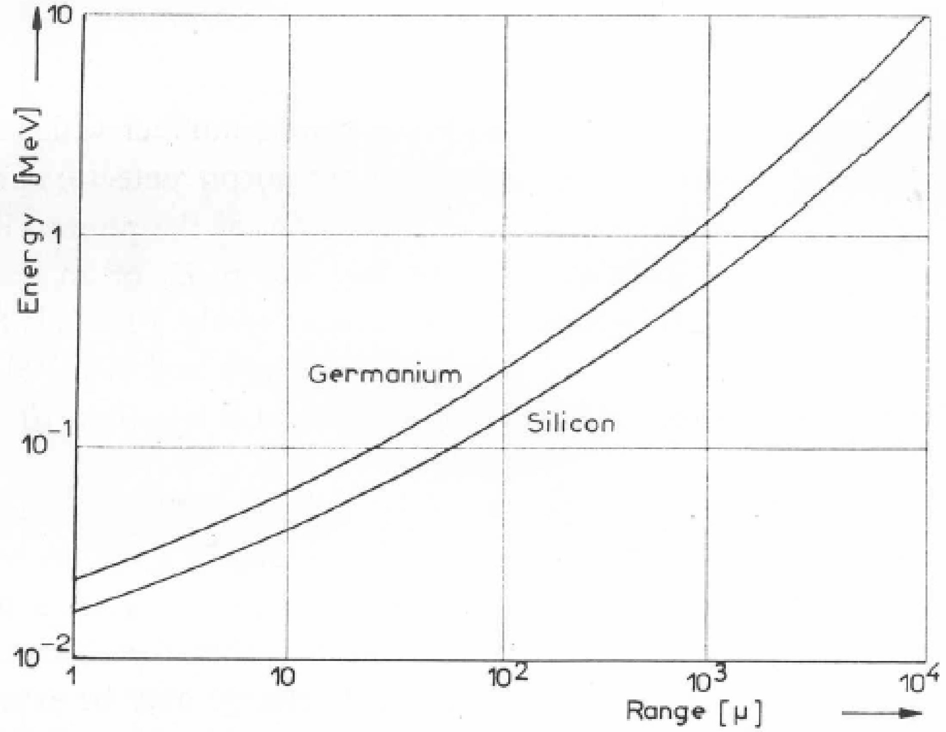

Fig. 4.1.10. Range versus energy for electrons in silicon and germanium.

Detection of photons and X-rays:

photon attenuation

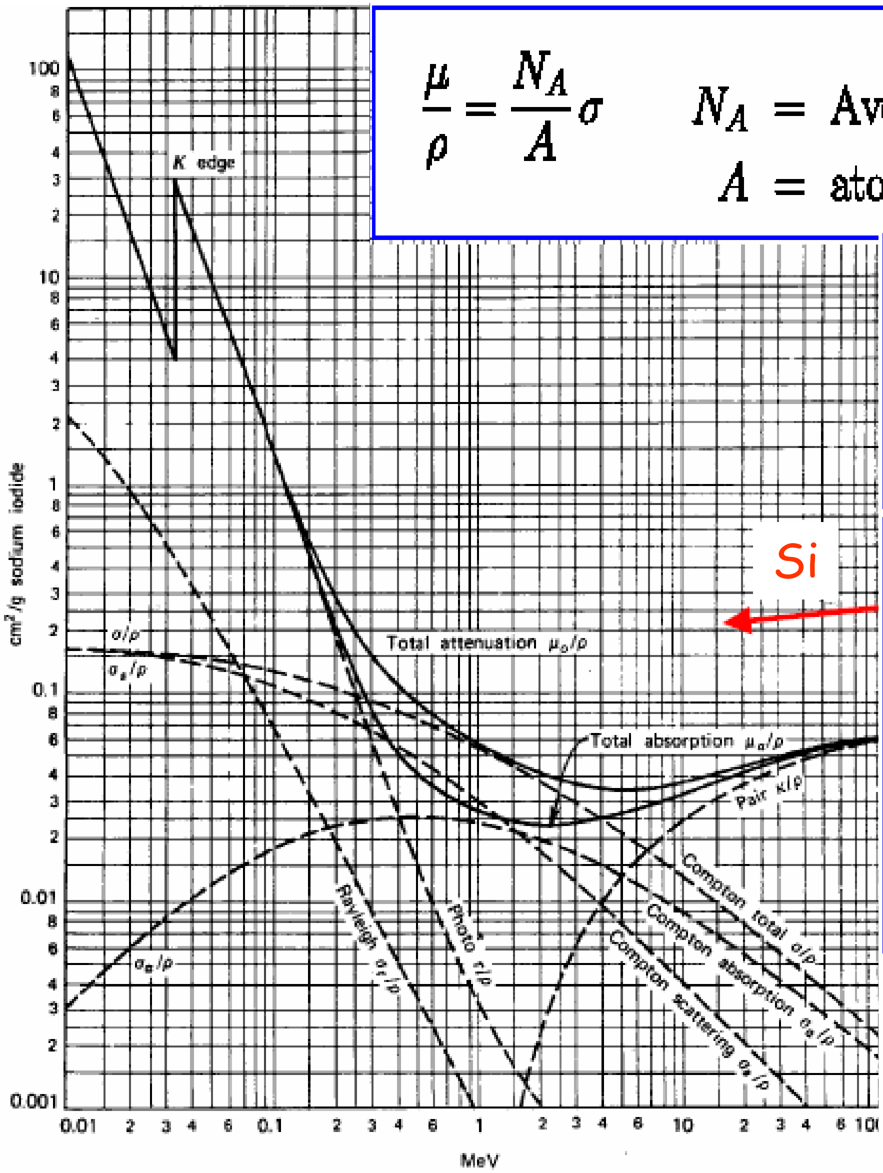

$$\frac{\mu}{\rho} = \frac{N_A}{A}\sigma \qquad N_A = \text{Avogadro's number}$$
$$A = \text{atomic mass of the absorber}$$

$$I = I_0 \exp(-\mu x)$$

μ = linear absorption coefficient

$$[\mu] = \mathrm{cm}^{-1}$$

$$\frac{1}{\mu} = \text{mean free path}$$

$\frac{\mu}{\rho}$ = mass attenuation coefficient
($\equiv \mu$ normalized by density ρ)

$$\left[\frac{\mu}{\rho}\right] = \frac{\mathrm{cm}^2}{\mathrm{g}}$$

$$\frac{\mu}{\rho} = \sum_i w_i \frac{\mu_i}{\rho_i}$$ for a mixture of elements with weight fractions w_i

$$\lambda = \frac{\rho}{\mu} = \text{mass attenuation length}$$

$$[\lambda] = \frac{\mathrm{g}}{\mathrm{cm}^2}$$

Detection of photons and X-rays: required detector thickness

Fraction of photons absorbed:

$$f = 1 - \exp(-\mu x)$$

Si and Ge can be used as efficient X-ray detectors for energies up to 30(100) keV

for higher energies high-Z detectors (eg CdTe, …)

10 keV photons in Si :

$\mu = 10^2\ \mathrm{cm}^{-1}$

$x = 300\ \mu\mathrm{m}$

$\mu x = 3,\ f = 0.95$

(photoabsorption)

1 MeV photons in Si :

$\mu = 10^{-1}\ \mathrm{cm}^{-1}$

$x = 30\ \mathrm{mm}$

$\mu x = 3,\ f = 0.95$

(Compton scattering)

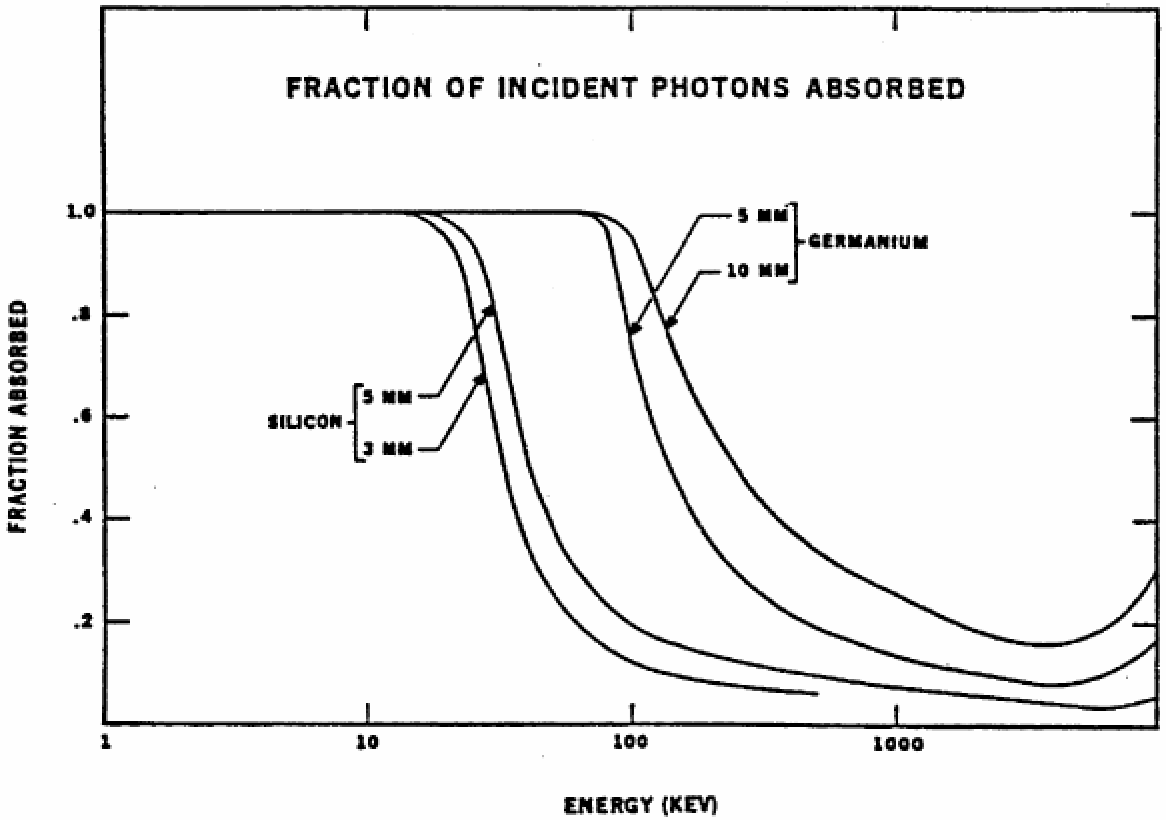

$\longrightarrow$ Better efficiency with Ge or higher Z

Detection of photons and X-rays: energy resolution – Fano factor

- mean number of charges for energy deposit E_0:

  $N_Q = E_0/\varepsilon$ (ε … energy required for e-h-pair)

- fluctuations: $\delta N_Q = \sqrt{F \cdot N_Q}$

  - if all N_Q ionizations independent → $F = 1$
  - constraints due energy conservation → $F < 1$

(simple model U.Fano Phys.Rev.72(1947)26 with a number of ad hoc assumptions:

  $F = E_X/E_{Gap} \cdot (\varepsilon/E_{Gap} - 1)$ (E_X … mean energy of phonon excitation, E_{Gap} … band gap)

- example Si:
  - $E_{Gap} = 1.1$ eV
  - $E_X = 0.037$ eV
  - $\varepsilon = 3.6$ eV

$F = 0.08$

$\delta N_Q = 0.3\sqrt{N_Q}$

significant im-
provement of δE

Chapter 3: Basics of Solid State Detectors

3.1 Principle

- Solid State Detectors are ionization chambers

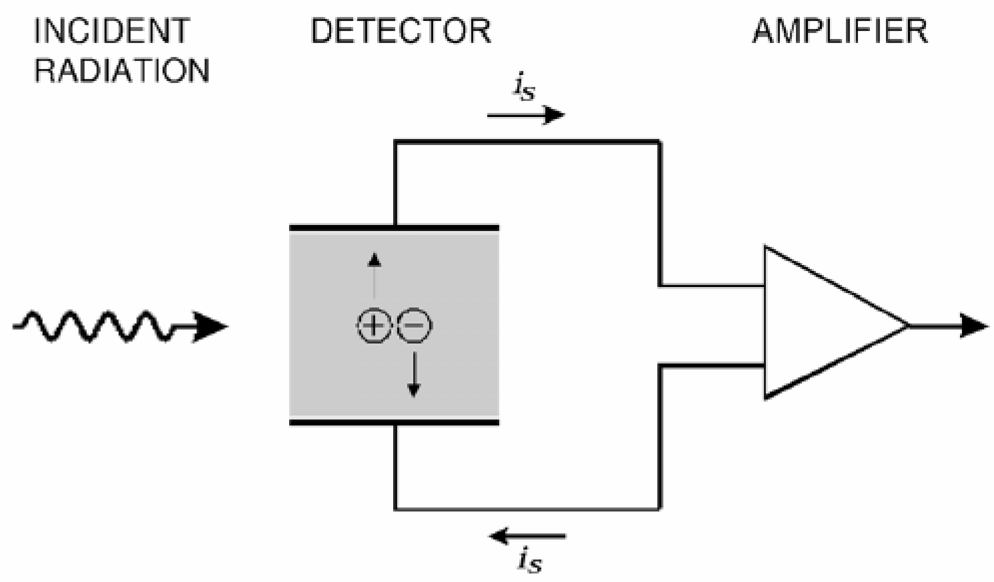

- any material which allows charge collection can be used for an ionization chamber
  - energy required to "ionize" (produce one charge pair):
    - ~30 eV for gases and liquids
    - 1-5 eV for solid state detectors
    - few meV to break up cooper pairs (and to produce phonons)

→ advantages solid state d.: efficient, density, room temperature operation, highly developed μ-technology, robust devices, well suited for μ-electronics readout

3.2 Semiconductor Properties

- Classification of conductivity:
- Diamond, Si, Ge have diamond lattice

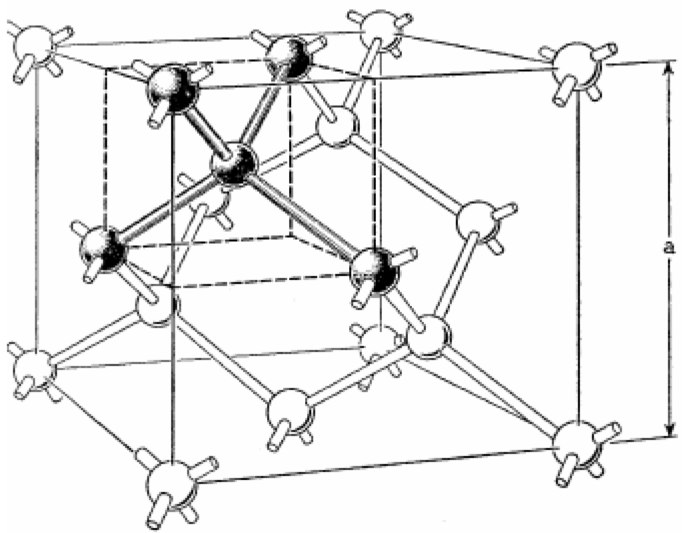

a = Lattice constant

Diamond:	a = 0.356 nm
Ge:	a = 0.565 nm
Si:	a = 0.543 nm

- crystalline structure

→ formation of electronic band gaps

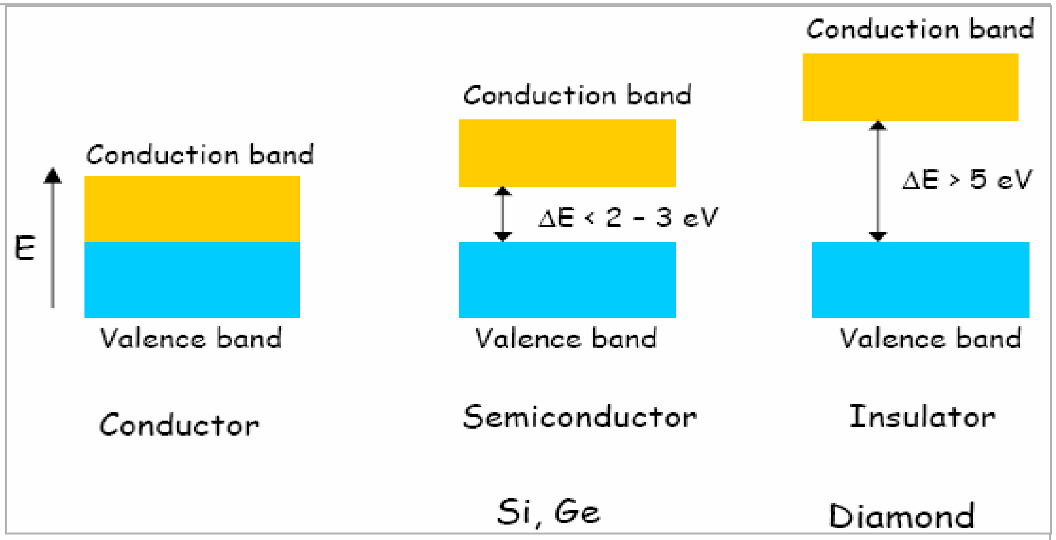

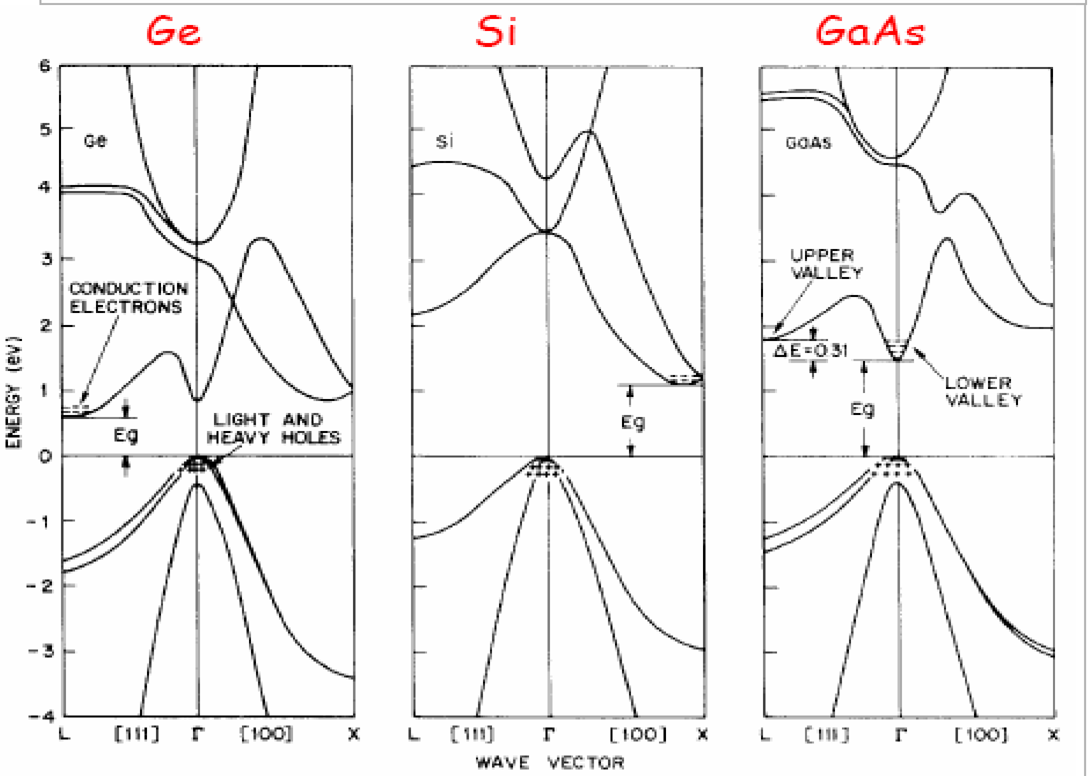

E_g = 0.7 eV E_g = 1.1 eV E_g = 1.4 eV

Semiconductor properties

- absorption photon → breaks bond → excite **electron in conduction band** and vacant **"hole" in valence band**
- electrons and holes move quasi freely in lattice (hole filled by nearby electron, thus moving to another position)

Property		Si	Ge	GaAs	Diamond
Atomic Number		14	32	31/33	6
Atomic Mass	[amu]	28.1	72.6	144.6	12.6
Band Gap	[eV]	1.12	0.66	1.42	5.5
Radiation Length X_0	[cm]	9.4	2.3	2.3	18.8
Average Energy for Creation of an Electron-Hole Pair	[eV]	3.6	2.9	4.1	~ 13
Average Energy Loss dE/dx	[MeV/cm]	3.9	7.5	7.7	3.8
Average Signal	[$e^-/\mu m$]	110	260	173	~ 50
Intrinsic Charge Carrier Concentration	[cm^{-3}]	$1.5 \cdot 10^{10}$	$2.4 \cdot 10^{13}$	$1.8 \cdot 10^{6}$	$< 10^{3}$
Electron Mobility	[cm^2/Vs]	1500	3900	8500	1800
Hole Mobility	[cm^2/Vs]	450	1900	400	1200

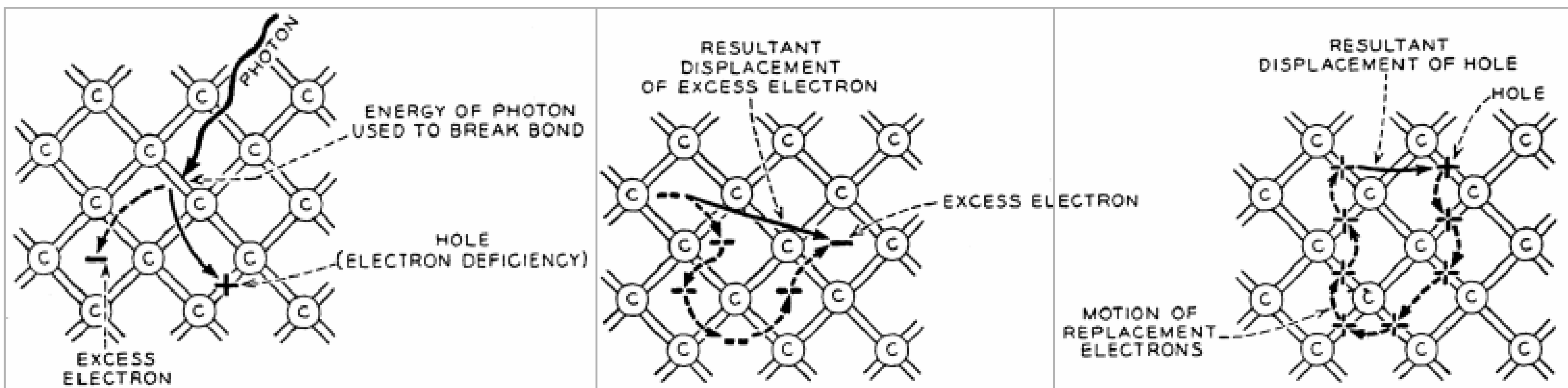

(a) PRODUCTION OF A HOLE-ELECTRON PAIR BY A PHOTON

(C) RANDOM MOTION OF AN EXCESS ELECTRON

(d) RANDOM MOTION OF A HOLE

- number of thermally excited charge carriers ($n_{intrinsic}$): $n_i = \sqrt{n_V n_C} \cdot \exp\left(-\frac{E_{Gap}}{2kT}\right)$

→ **Si at room temperature (kT ~ 26 meV): 1.5 10^{+10} cm^{-3} (10^{-12} !)**

Mobility μ: electrons and holes drift under the influence of electric field E:

- for low fields (Si < 5kV/cm)

  $\vec{v} = \mu\,\vec{E},\ \mu$ ... mobility
- for high fields v ~ 10^7cm/s

→ charge collection times for 300µm Si detector: $\mathcal{O}$(10ns)

- drift in magnetic field

→ Lorentz angle: $\tan\theta = \mu_{Hall} \cdot B_T$

Hall mobility:

electrons: μ_{Hall}=1650cm²/Vs

holes μ_{Hall} = 310cm²/Vs

→ ~30° for 4 Tesla field (e)

(165 µm shift for 300 µm)

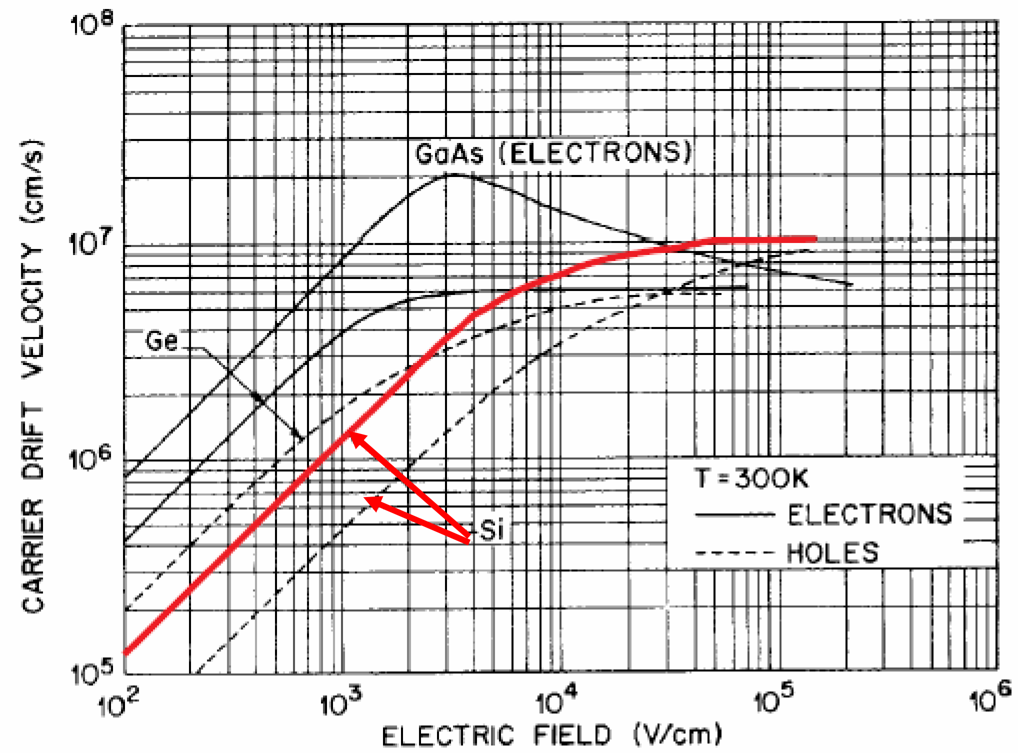

Diffusion D:

- Einstein relation: $D = (kT/q) \cdot \mu$

→ spread of charge after time t:

$\sigma^2 = 2 \cdot D \cdot t$

→ 6 µm for 10ns drift of electrons

Resistivity ρ: defined by $\vec{E} = \rho \cdot \vec{J}$ (*J* ... current density)

for semiconductors with both electrons (*n*) and holes (*p*) as carriers: $\rho = \dfrac{1}{q(\mu_n \cdot n + \mu_p \cdot p)}$

n ... density of electrons, *p* ... density of holes

→ resistivity of intrinsic Si at room temperature: 230 kΩ cm

Doping of Semiconductors

By addition of impurities (doping) the conductivity of semiconductors can be tailored:

By doping with elements from group V (Donator, e.g., As, P) one obtains n-type semiconductors

One valence electron without partner, i.e. impurity contributes excess electron

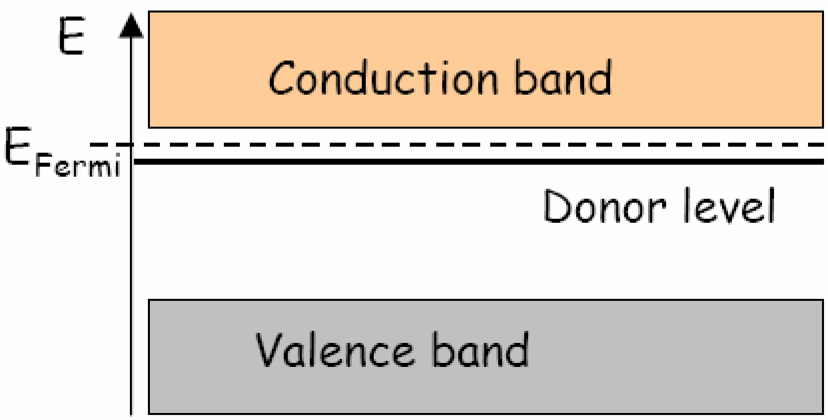

By doping with elements from group III (Acceptor, e.g., B) one obtains p-type semiconductors

One Si valence electron without a partner, impurity borrows an electron from the lattice

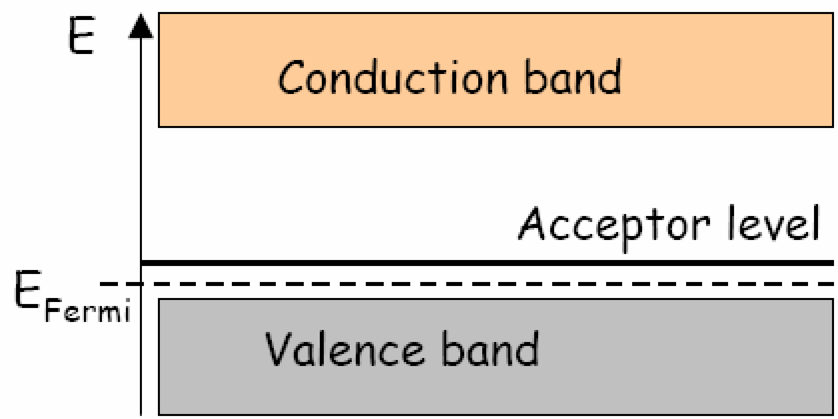

$E_{D,A}$ ~ 10meV → ionized at room temp (25meV)

→ resisitivity dominated by majority charge carriers $n = N_{D,A}$: $\rho = 1/(q\,\mu_i n_i)$

typical doping concentrations (Si):

detectors: few 10^{12}cm^{-3} → ρ = 1 … 5 kΩcm

electronics: O(10^{16}cm^{-3}) → ρ = O(Ωcm)

Doping of Semiconductors

The excess electrons are only loosely bound, since the Coulomb force is reduced by the dielectric constant ε of the medium:

$$E_i(\text{lattice}) = E_i(\text{atom})/\varepsilon^2$$

The impurity levels are in the order of 10 meV above or below the band edges

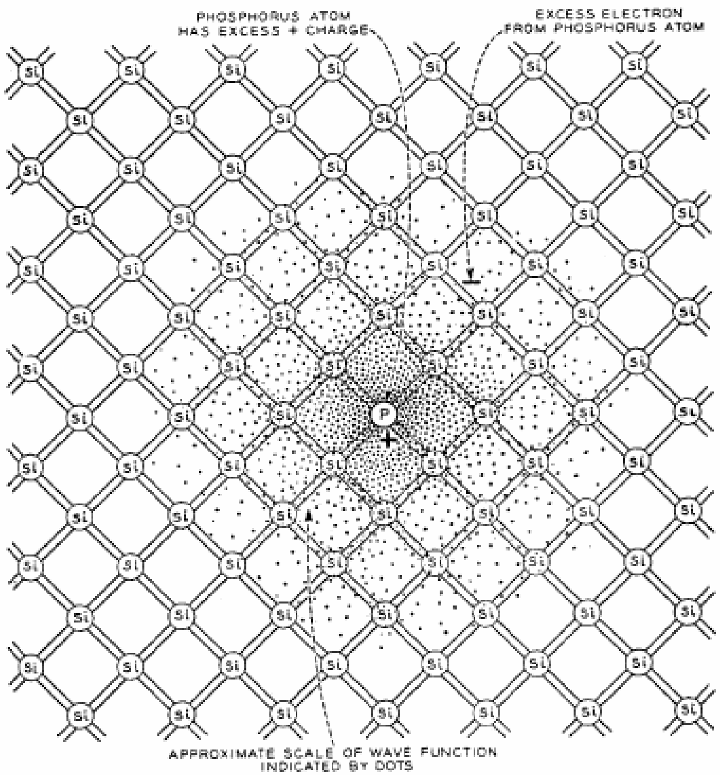

The wavefunction of the dopants extends over many neighbours

3.3 How to build a solid state ionization chamber – the pn junction

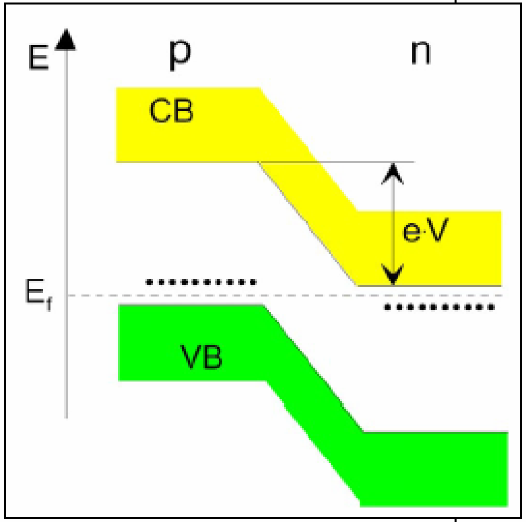

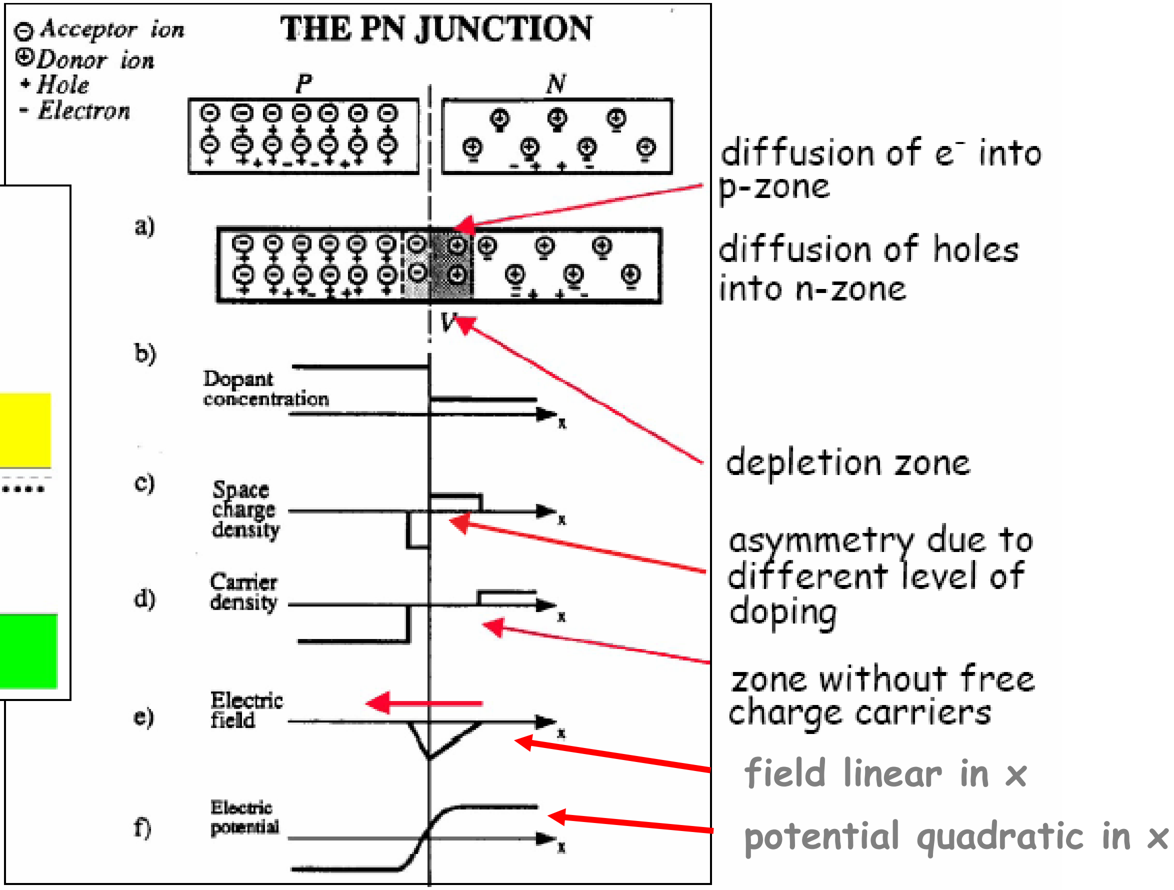

- thermal diffusion drives electrons and holes across pn junction

→ generation of depletion regions (no free charge carriers) with fixed space charge

- potential and electric field obtained from Poisson's equation: $-\frac{d^2V}{dx^2} = \frac{dE}{dx} = \frac{\rho(x)}{\varepsilon}$

- diffusion potential (built-in potential V_{bi}) obtained by E_{Fermi} = const over junction
  for Si one-sided abrupt junction $V_{bi} \sim 0.65$V for n doping few $1.4 \cdot 10^{+12}$cm^{-3} (3 kΩcm)
  → depth of depletion region: d ~ 25 μm

pn junction with backward bias:

- apply bias voltage V_b to "help" diffusion voltage V_{bi}
- depletion width obtained from:
  - Poisson's equation (one dimension, const. charge density): $V_b + V_{bi} = \frac{q}{2\varepsilon}(N_D x_n^2 + N_A x_p^2)$
  - charge neutrality: $N_D x_n = N_A x_p$

  → depletion width: $W = x_n + x_p = \sqrt{\frac{2\varepsilon(V_b + V_{bi})}{q}\left(\frac{1}{N_A} + \frac{1}{N_D}\right)}$

- for detectors highly asymmetric junctions are chosen, eg p^+n ($N_A \gg N_D$)

  → depletion region $x_n \gg x_p$, and: $W \approx x_n = \sqrt{\frac{2\varepsilon(V_b + V_{bi})}{q N_D}} = \sqrt{2\varepsilon\mu_n\rho_n(V_b + V_{bi})}$

  (usually $V_b \gg V_{bi} \sim 0.65$ V in Si)

  → detector capacitance given by region free of mobile charges: $C = \varepsilon\frac{A}{W} = A\sqrt{\frac{\varepsilon q N_D}{2V_b}}$

  (standard method to experimentally determine N)

if W ≥ detector thickness D

→ fully depleted detector

(entire volume sensitive)

for D = 300μm, n-type

ρ = 3 kΩcm

→ $V_b = V_D = 100$ V

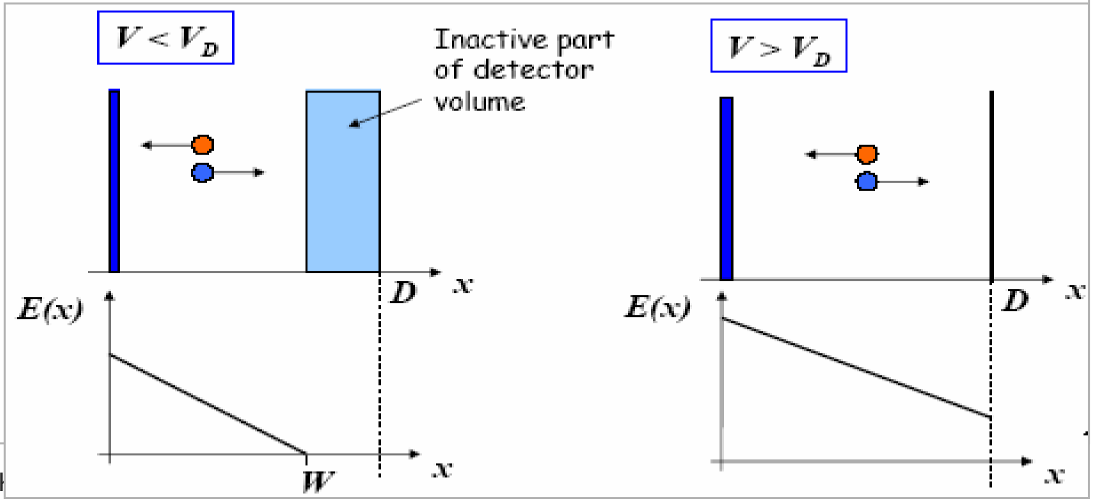

electric field in over-depleted pn junction and charge collection time:

- depletion voltage: $V_D = \frac{q N_D}{2\varepsilon} D^2$

- electric field at x = D: $E(D) = (V_b - V_D)/D$

$\rightarrow$ $$\boxed{E(x) = \frac{2V_D}{D}\left(1 - \frac{x}{D}\right) + \frac{V_b - V_D}{D}}$$

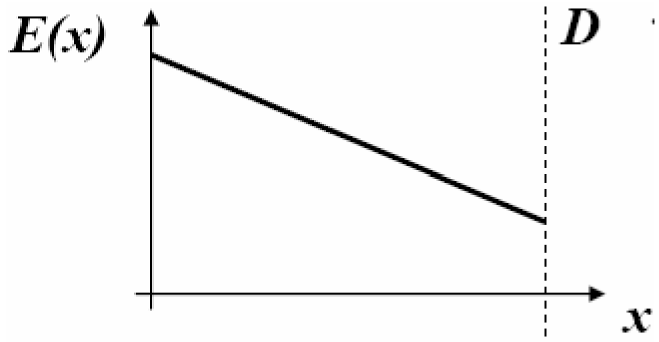

- drift: $v(x) = \mu E(x) \rightarrow t(x_1, x_2) = \int_{x_1}^{x_2} \frac{dx}{v(x)}$

- time needed for charge carriers to traverse entire detector: $$\boxed{t_{drift} = \frac{D^2}{2\mu_i V_D} \ln\left(1 + \frac{2V_D}{V_b - V_D}\right) \xrightarrow{V_b \gg V_D} \frac{D^2}{\mu_i V_b}}$$

$\rightarrow$ for D = 300μm, n-type
ρ = 3 kΩcm, V_b = 200 V: $t_{drift}(n)$ = 3.5 ns, $t_{drift}(p)$ = 11 ns

3.4 Signal formation in planar pn diode:

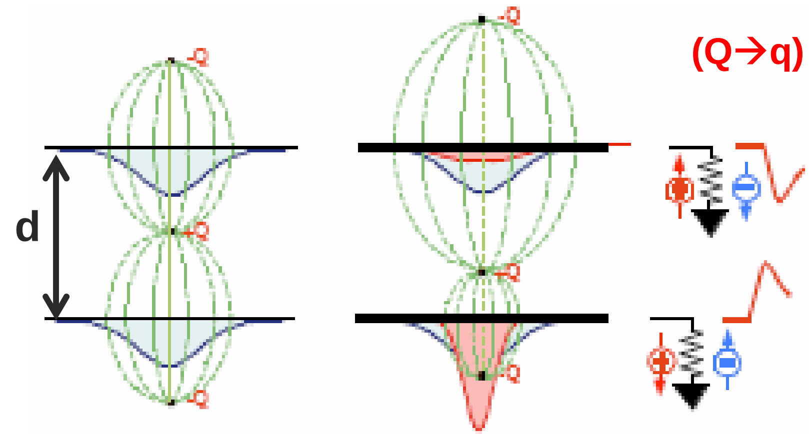

- signal in electrodes by induction
  (not arrival of charge at electrodes !)
- electrodes (example parallel plates)
  via low Z amplifier at const. potential
- electrostatic problem can be solved
  by ∞ no. of image charges
- moving charge changes charge profile
  → induces detectable signal
- problem can also (and best) be solved by method of weighting fields

  -example: charge pair +/-q produced at x_0

- induced current: $$I = \frac{dQ}{dt} = -q\frac{v}{d}$$

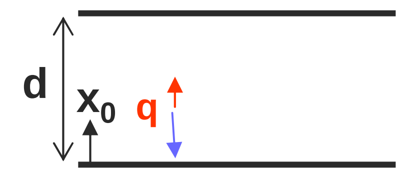

- total charge
  induced by -q $$Q^- = -\frac{-q}{d}\int_{x_0}^{d} dx = -\frac{q}{d}x_0$$

  induced by +q $$Q^+ = -\frac{+q}{d}\int_{x_0}^{0} dx = -\frac{q}{d}(d - x_0)$$

  sum $$Q = Q^- + Q^+ = -q$$

(total charge q independent of starting point x_0)

- situation more complicated when electrodes are segmented (eg strip detectors)

Example: pulse shape in strip detector

detector properties: ρ = 5kΩcm, V_b = 200V, D = 280 μm, d = 100 μm strips, x_0= 140 μm

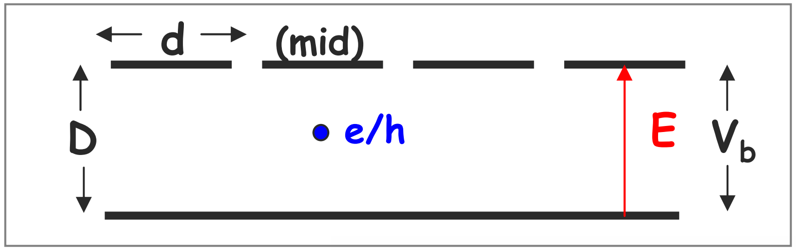

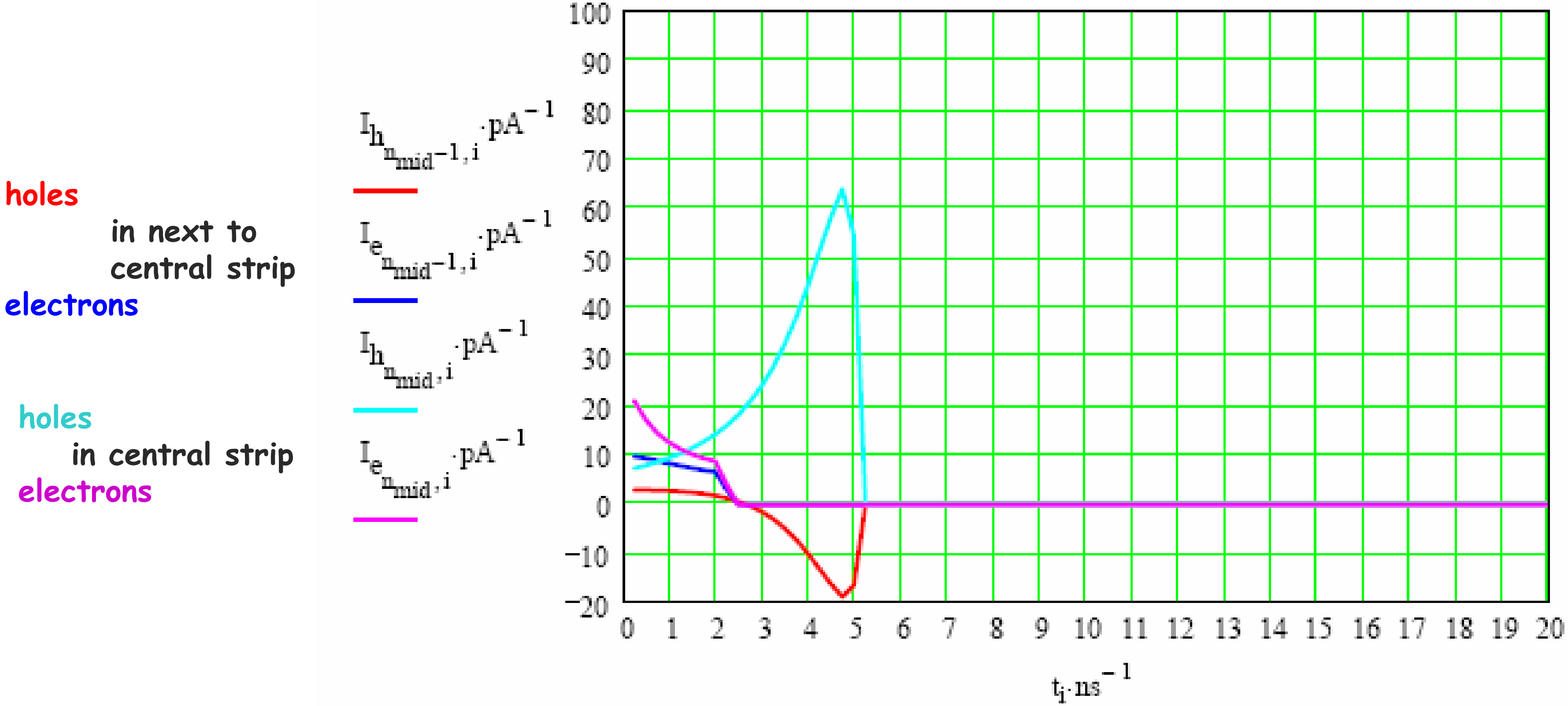

3.5 Detector Fabrication (J.Kemmer NIM 169(1980)449)

Steps in the Fabrication of Planar Silicon Diode Detectors

Polishing and cleaning

Oxidation at 1300 K

Deposition of photosensitive polymer, UV illumination

Creation of p-n junction via implantation/diffusion

Annealing: implanted ions occupy lattice sites

Deposition of Al and

patterning for electric contacts

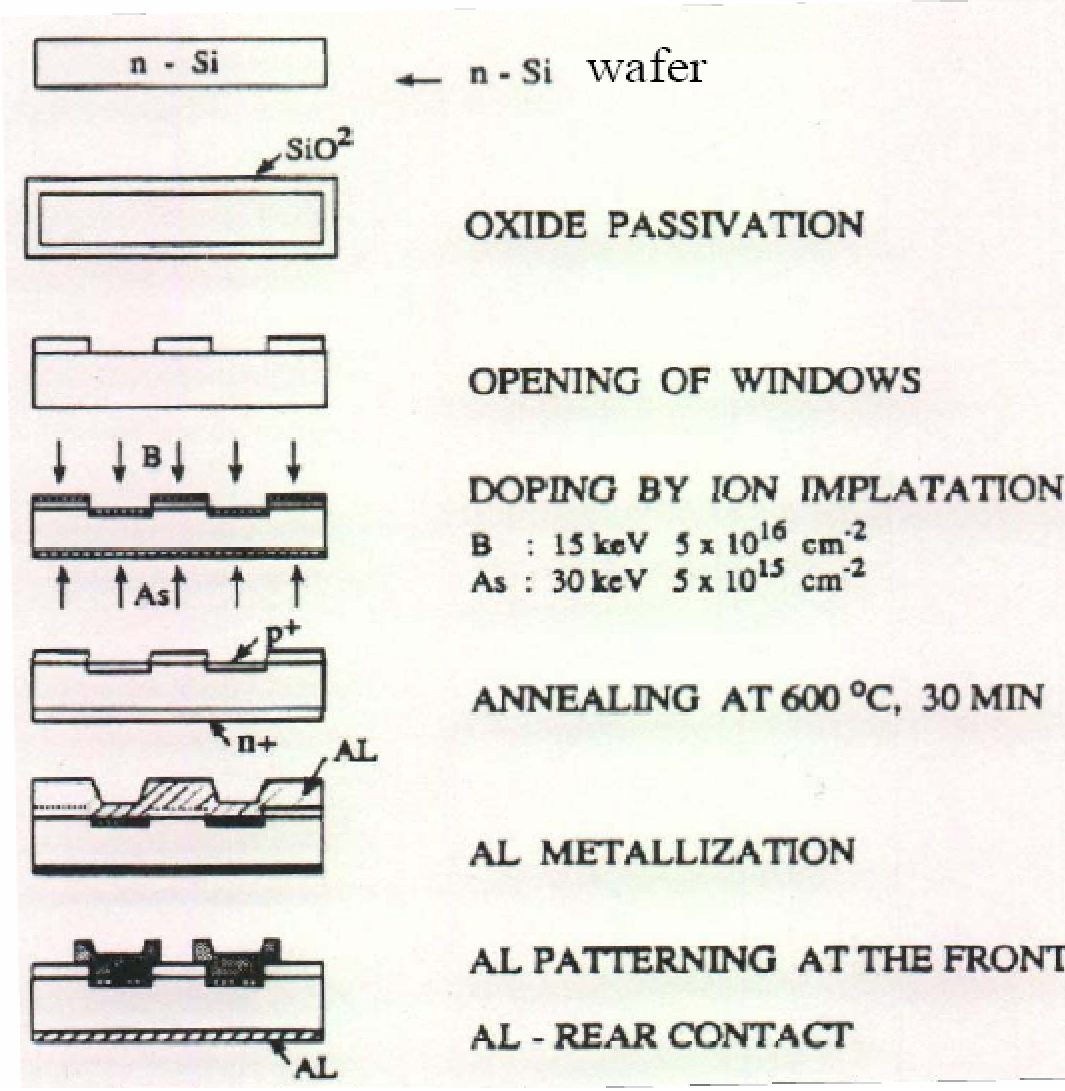

Ch.4 Detector Types

Solid state detectors:

- "efficient" (Si: 3.6 eV/e-h pairs) + high density → large signal
- high speed (~ 10 nsec)
- highly developed technology (micro-electronics) → accuracy (μm) + reliability (if properly designed !)
- reasonably rad.hard (~10^{15}n/cm^2)
- possibility to integrate electronics
- no internal gain needed → stability

but: limited size + fairly high cost

4.1 Low Noise Electronics

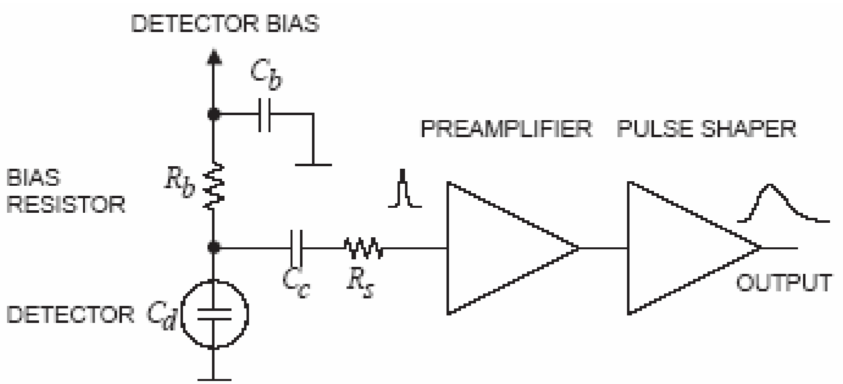

Typical detector front-end circuit.

- most detectors rely critically on fast low-noise electronics
- major progress due to development of low-power/low-noise micro-electronics
  - C_d … detector (model – R_d !)
  - R_b … biasing resistor
  - C_C … blocking capacitor
  - R_S … all resistors in input path
- model (equivalent circuit) for noise analysis:

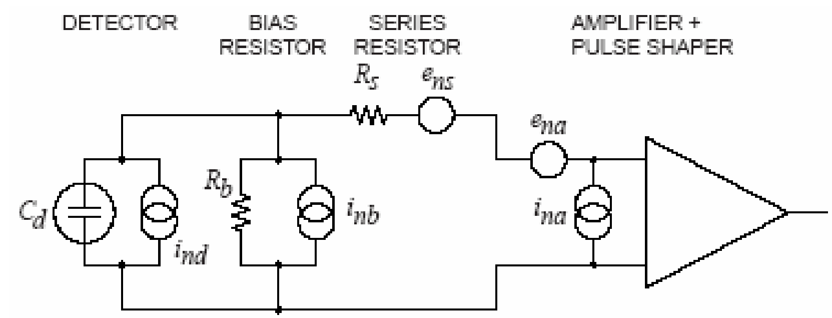

- i_{nd} … leakage current (det. noise)
- i_{nb} … R_b shunt resistor noise
- i_{na} … amplifier current noise
- e_{ns} … series resistor voltage noise
- e_{na} … amplifier voltage noise

→ interplay detector -- read-out

- shot noise (amplitude)^2: $i_{nd}^2 = 2eI_d$
- thermal noise: $i_{nb}^2 = \frac{4kT}{R_b}$, $e_{ns}^2 = 4kTR_s$

  (I_d … detector bias current,
  typ. values: e_{na} nV/√Hz, i_{na} pA/√Hz)
  have a "white" frequency spectrum – constant $dP_n/df \propto di_n^2/df \propto de_n^2/df$

  in addition $e_{nf}^2 = \frac{A_f}{f}$ 1/f-noise due to charge trapping and de-trapping in resistors, dielectrics, semi-conduct… with typ.values A_f = $10^{-10}…10^{-12}V^2$)
- dark current detector → frequency dependent noise voltage $i_n/(\omega C_d)$
- individual noise contribution un-correlated → quadratic sum
- total noise at output: integration over the bandwidth of the system
- random noise → Gaussian spread
- noise expressed in equivalent noise charge Q_n (Coul,e) or in equivalent energy (eV)

frequently not easy to get rid of pick-up+… !!!

- for a capacitive sensor (→ p.1):

$$Q_n^2 = i_n^2 F_i T_S + e_n^2 F_v \frac{C^2}{T_S} + F_{vf} A_f C^2$$

total = current/parallel + voltage/serial + shot noise

C … sum of all capacitances at input
T_S… characteristic time amplifier
F_k… "form-factors" property amplif.
(W(t)… response to δ-function pulse)

$$F_i = \frac{1}{2T_S}\int_{-\infty}^{\infty}[W(t)]^2\,dt\ , \qquad F_v = \frac{T_S}{2}\int_{-\infty}^{\infty}\left[\frac{dW(t)}{dt}\right]^2 dt$$

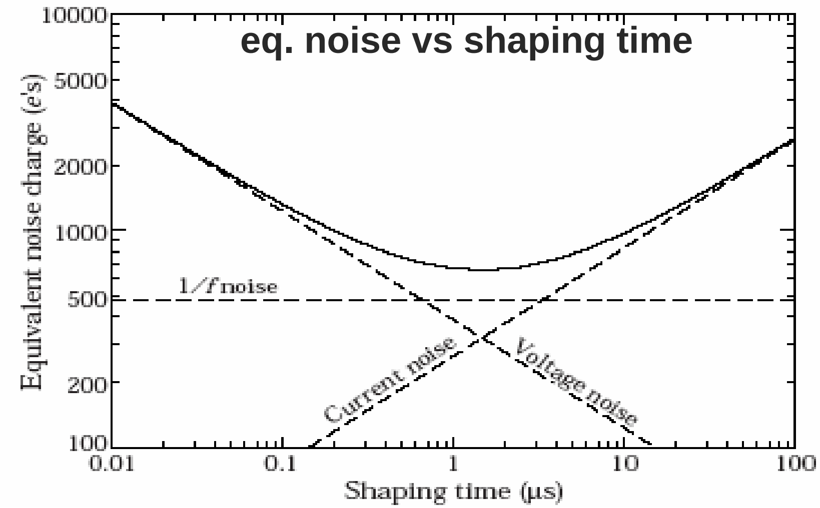

typical values achieved:
- 1e for CCDs
- few 10 … 100e for pixel detectors
- 1000e for strip detectors

4.2 Silicon Strip Detectors

- in 1980 started success story of Si-precision detectors in particle physics

single-sided readout

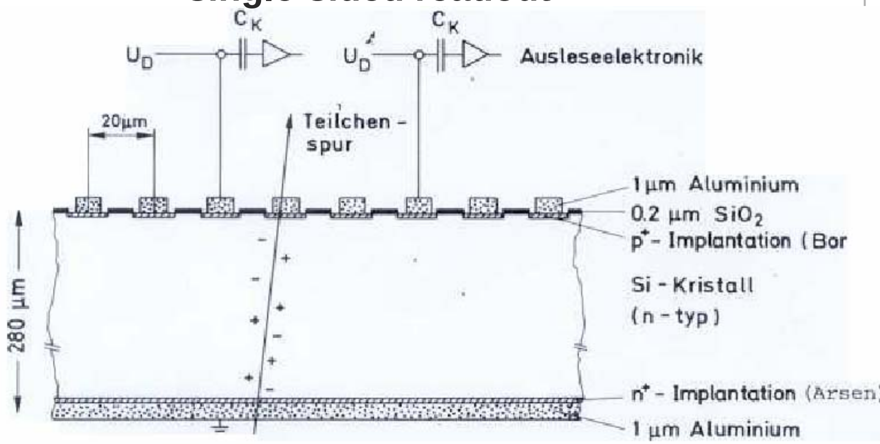

double-sided readout

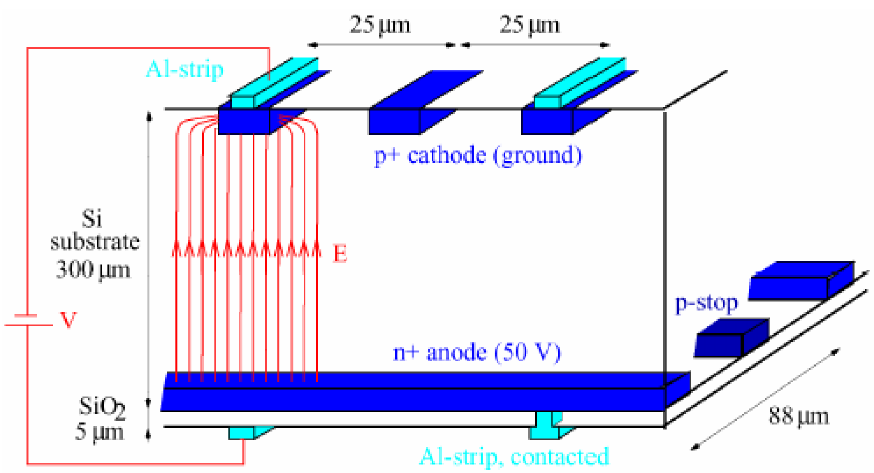

Special measures to avoid short-circuit on n^+-side (for n-type detectors):

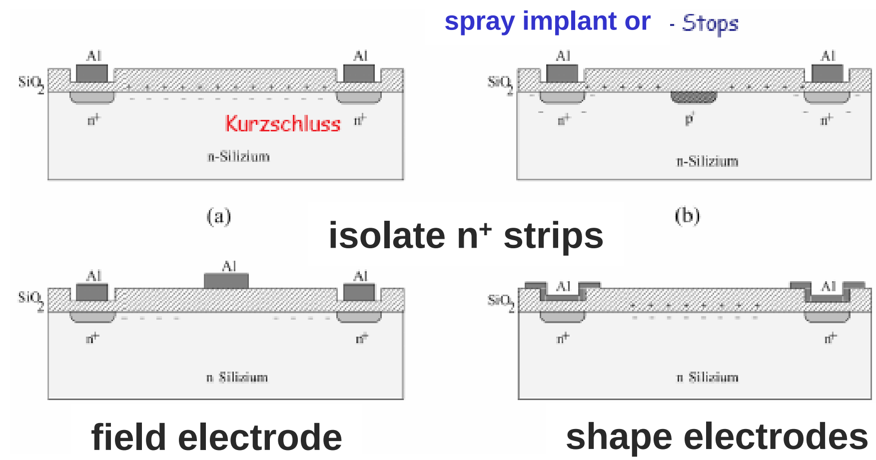

- example: H1 strip detector

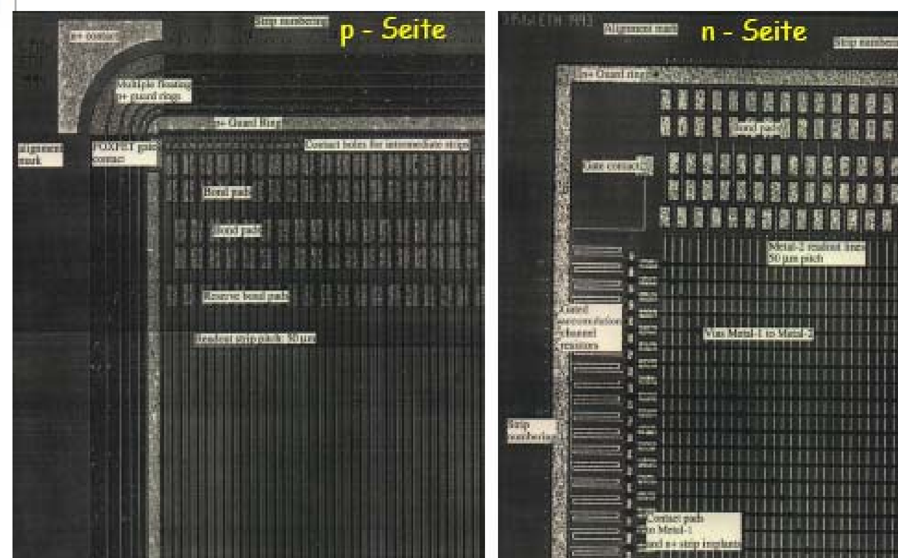

spatial resolution: strip pitch with interpolation by diffusion (~10 μm)

measured distribution of holes at p^+ strips

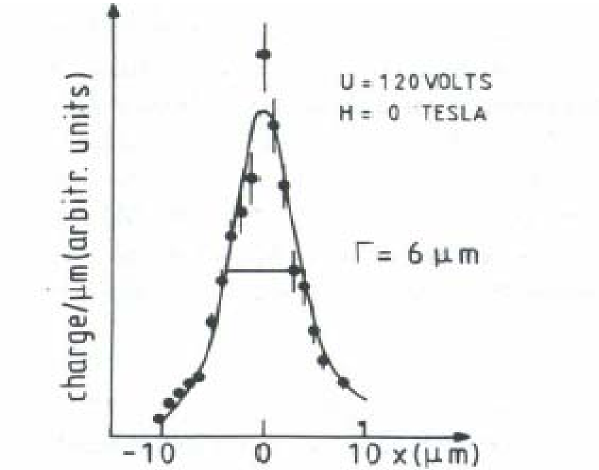

- coupling of detectors to reduce no. of readout channels (ladders)

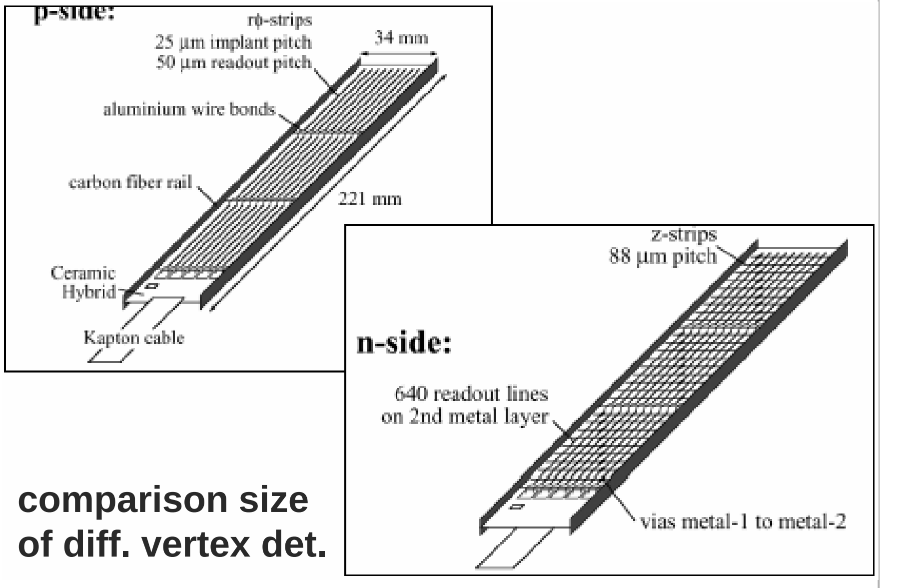

comparison size of diff. vertex det.

achieved resolution: ~ 1μm (detector with 20μm pitch NIM235(1985)210)

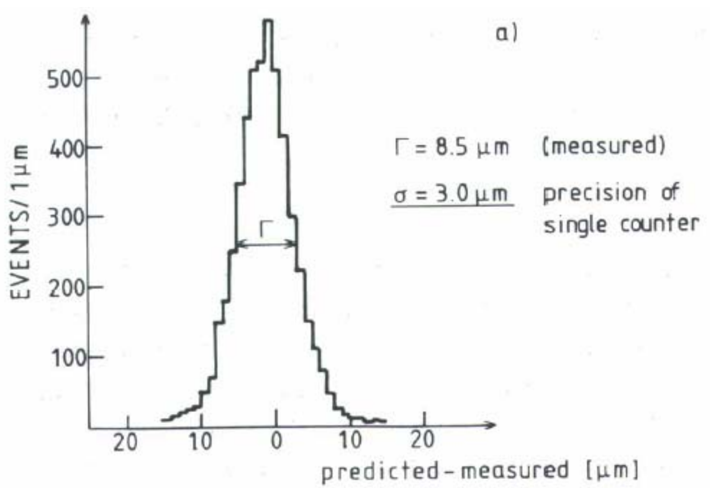

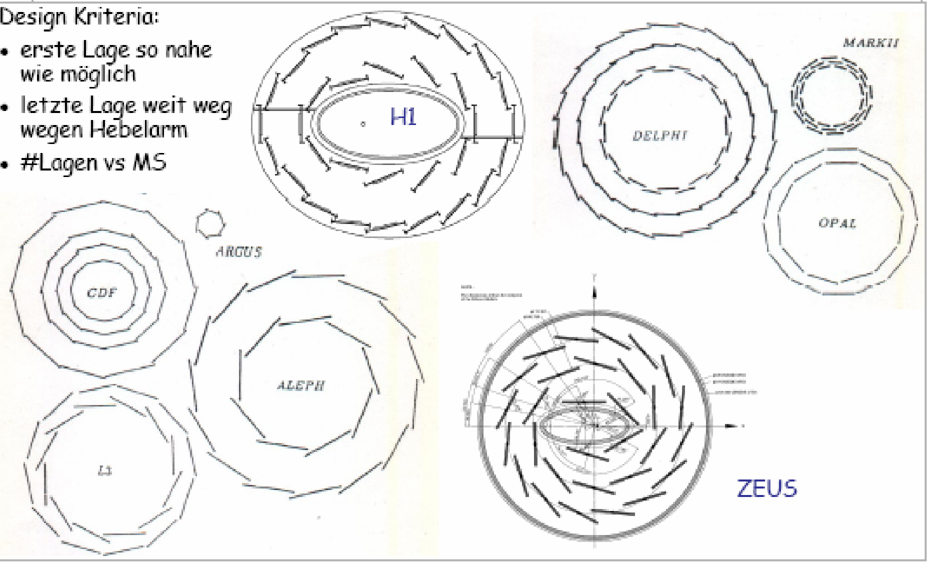

Si-vertex detectors: complex, high-tech detectors – e.g SVXII for CDF

Total 720000 Auslesekanäle

Installation inside CDF

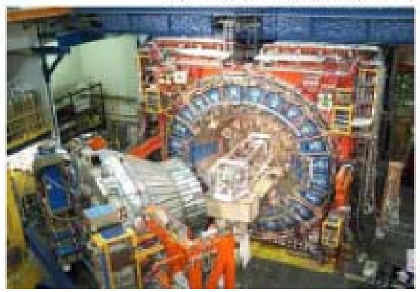

CMS-tracking: world's largest Si-det.!

2007: LHC@CERN

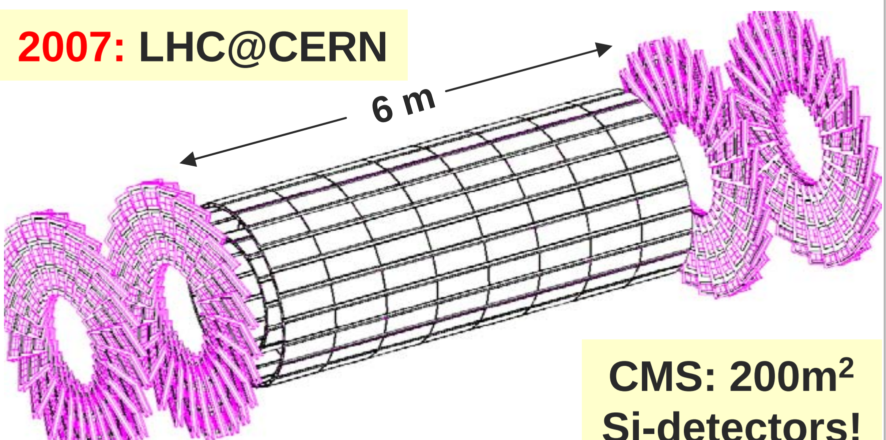

CMS: 200m^2 Si-detectors!

Si-vertex detectors at DESY (HERA):

H1 FST (Forward Silicon Tracker)

ZEUS MVD (MicroVertex Detector) at DESY

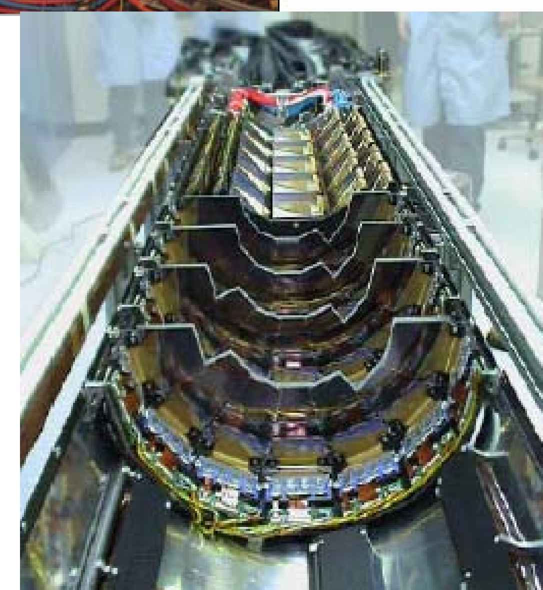

4.3 Solid State Drift Chambers

Principle (like back-to-back diodes):

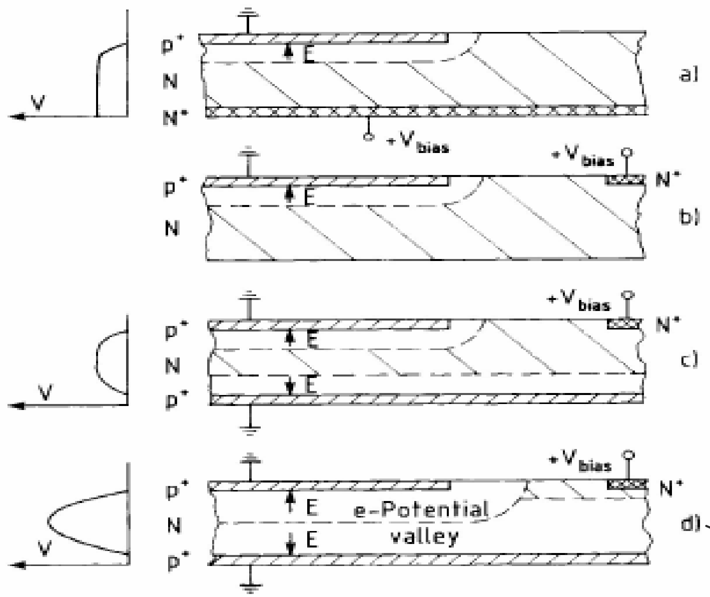

potential distribution

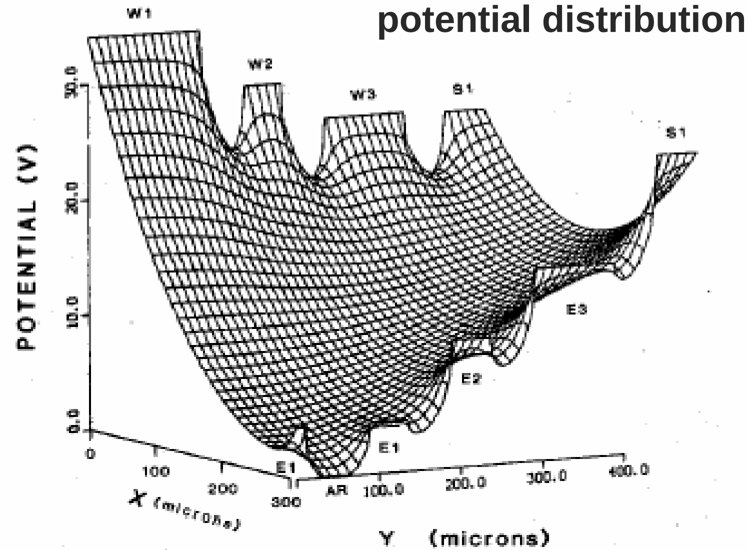

Fig. 4. Potential energy for electrons in the anode region. (Because of symmetry, only the region corresponding to the right part of the above cross section is shown.)

segmented anode → 2(3)-d measurement

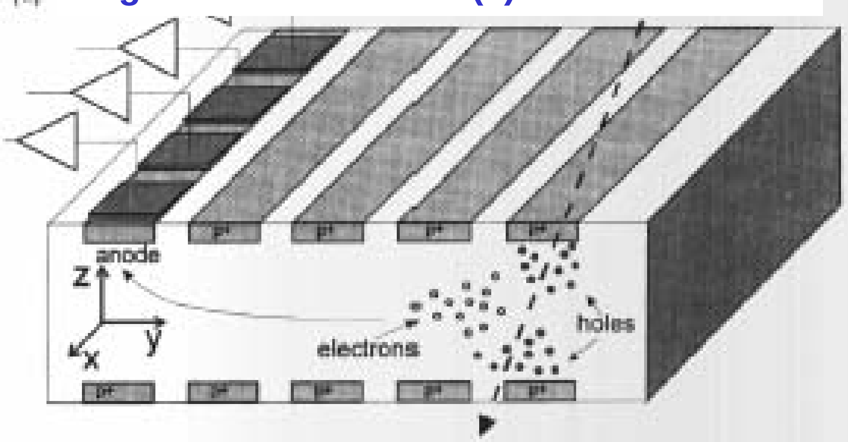

C-V characteristics of Si-drift chamber

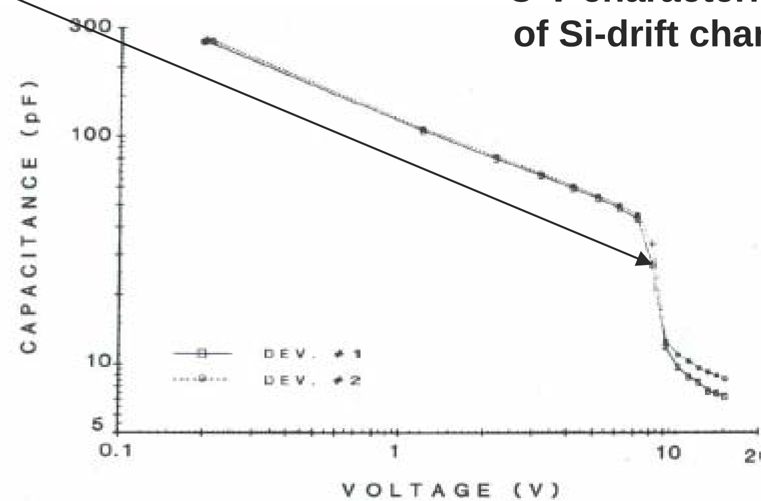

- first realisation (NIM235(1985)231)

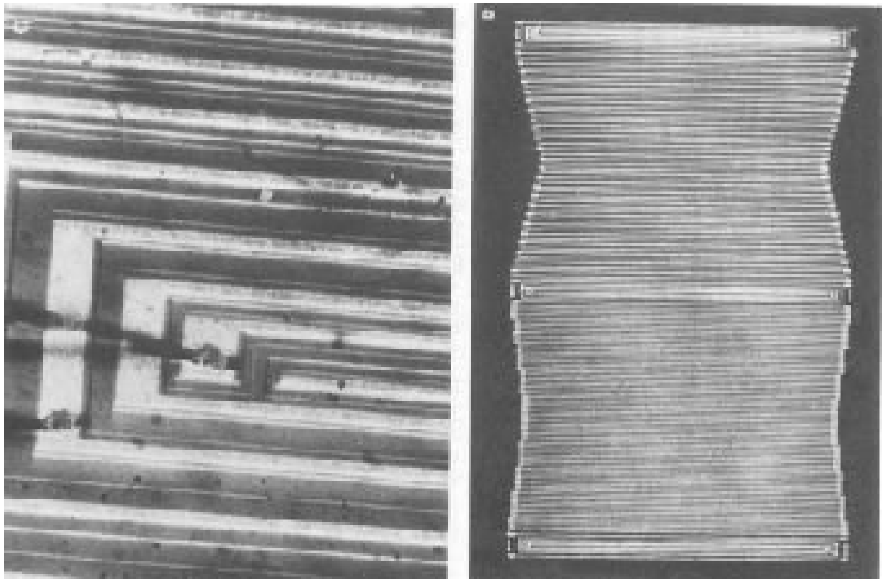

- position resolution vs drift field →
  ~ 5µm achieved

Laser spot

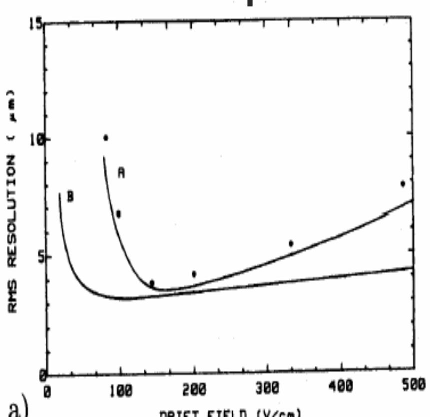

a)

beam particles

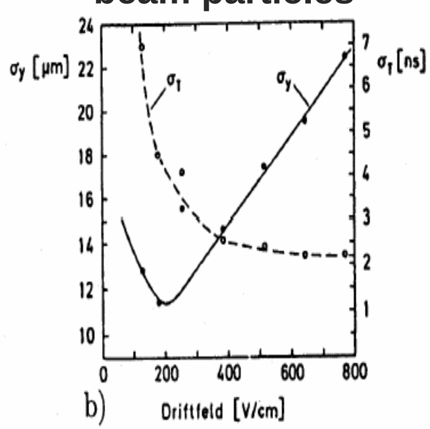

b)

example of a vertex detector based on Si-drift chambers (STAR detector at RHIC, BNL – NIMA 541(2005)57)

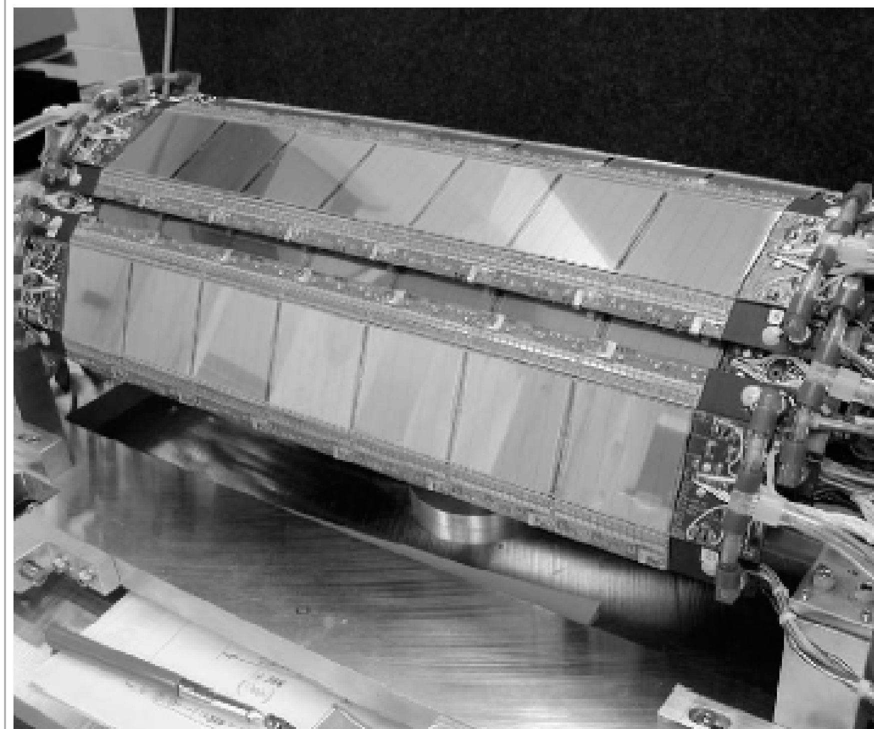

- excellent 2d position resolution with small no. of read-out channels **but**
- speed (several 100 ns drift times)
- sensitivity to radiation

drift principle → many applications!

high resolution X-ray detector:

to profit from low C: on detector FET

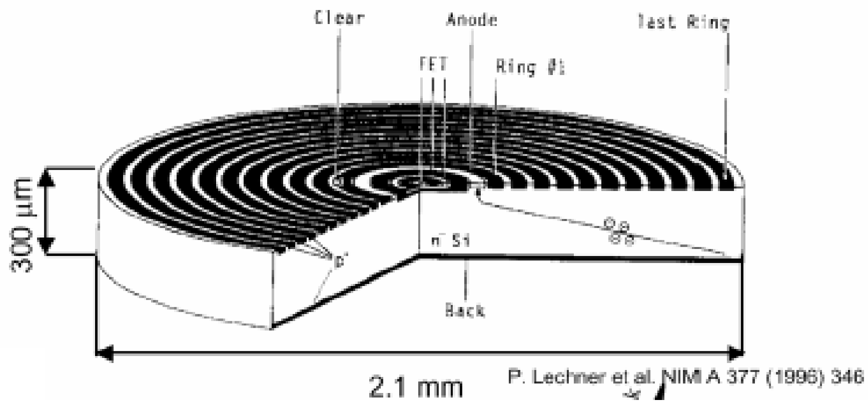

P. Lechner et al. NIM A 377 (1996) 346

energy resolution: 121eV@6keV (-10°)

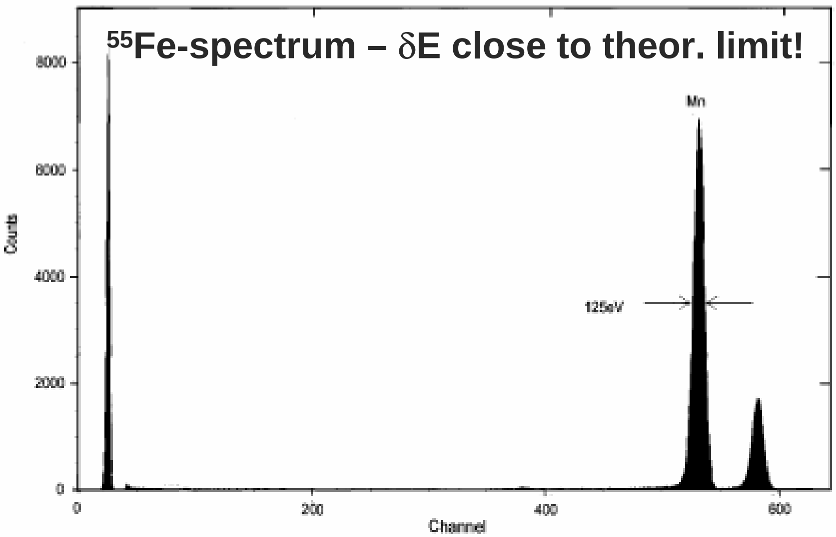

Pixel Detectors:

4.4 Charged Coupled Devices (CCD)

principle of operation:

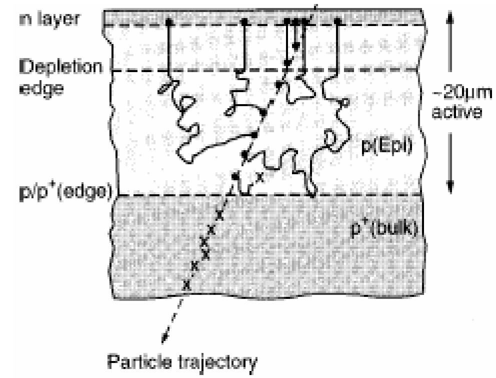

: 4. Charge collection within a buried-channel CCD structure.

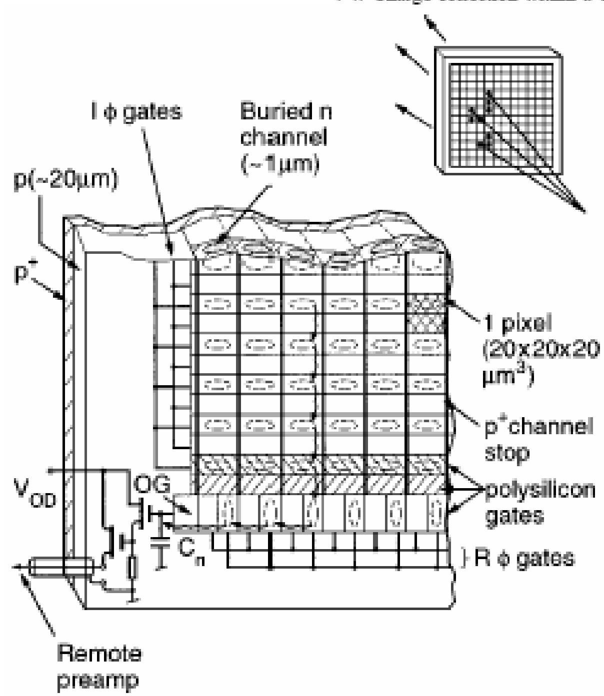

CCD principle of operation

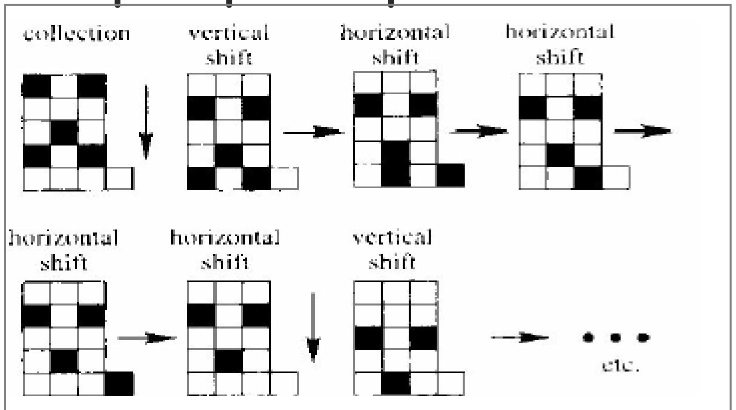

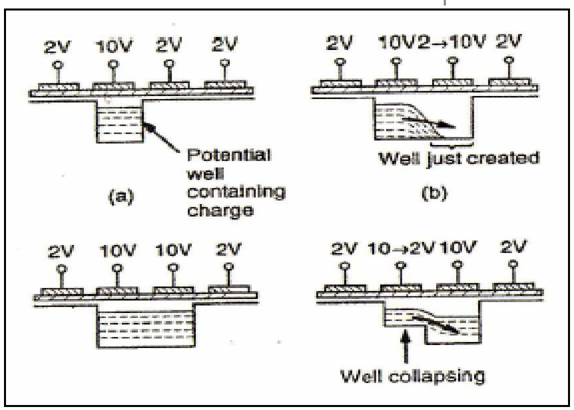

- many (10^6) pixels – small no. of channels
- excellent noise performance (few e)
- small pixel size (e.g. 22x22 μm^2)
- slow (many ms) readout time
- sensitive during read-out
- radiation sensitive

→ used at SLC → best vertex detector so far with 3×10^8 pixels !!!

technological realisation:

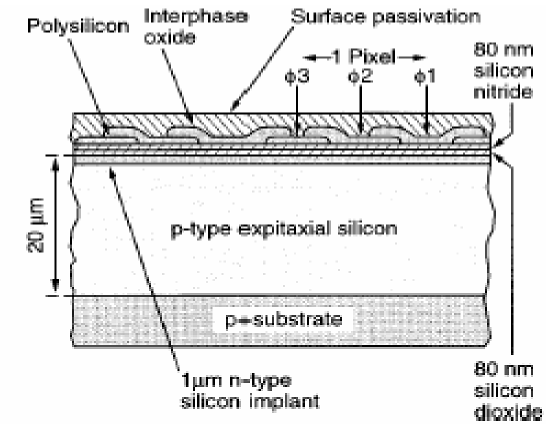

FIG. 6. Gate structure of a modern three-phase CCD register designed to avoid potential wells due to radiation-induced charge buildup or other spurious charge in the dielectric or surface-passivation layers.

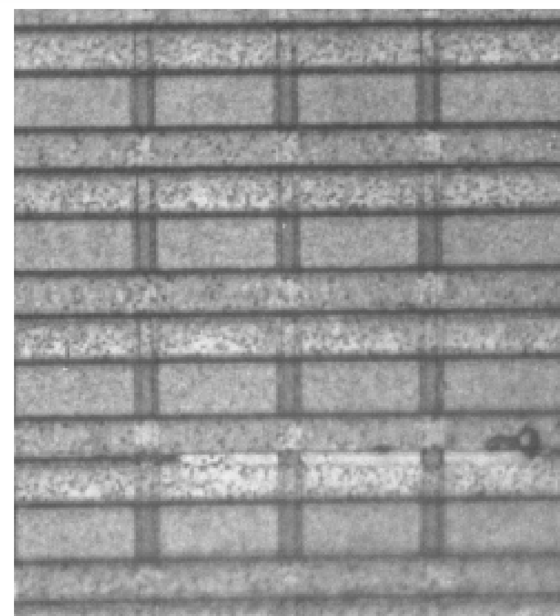

SLC Vertex detector:

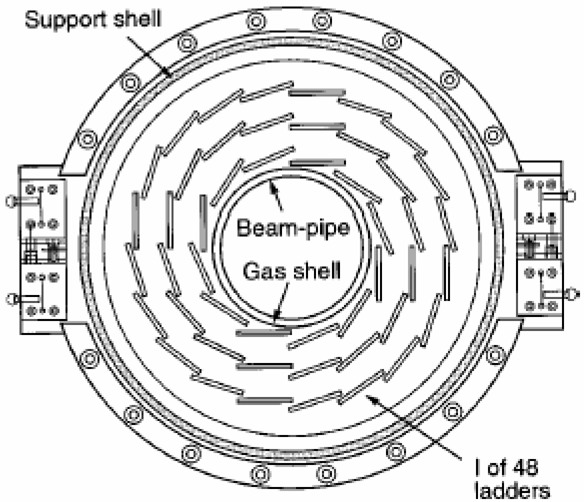

FIG. 18. Cross section (end view) of the VXD3 detector.

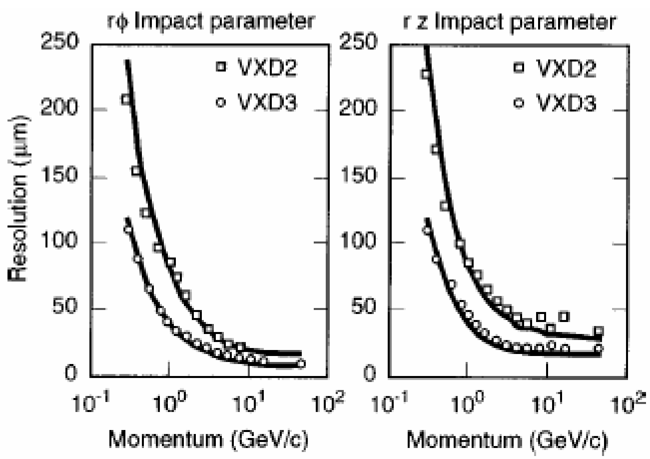

FIG. 20. Measured impact parameter resolution as a function of track momentum for tracks at cos θ=0 for VXD2 and VXD3 compared with the Monte Carlo simulations.

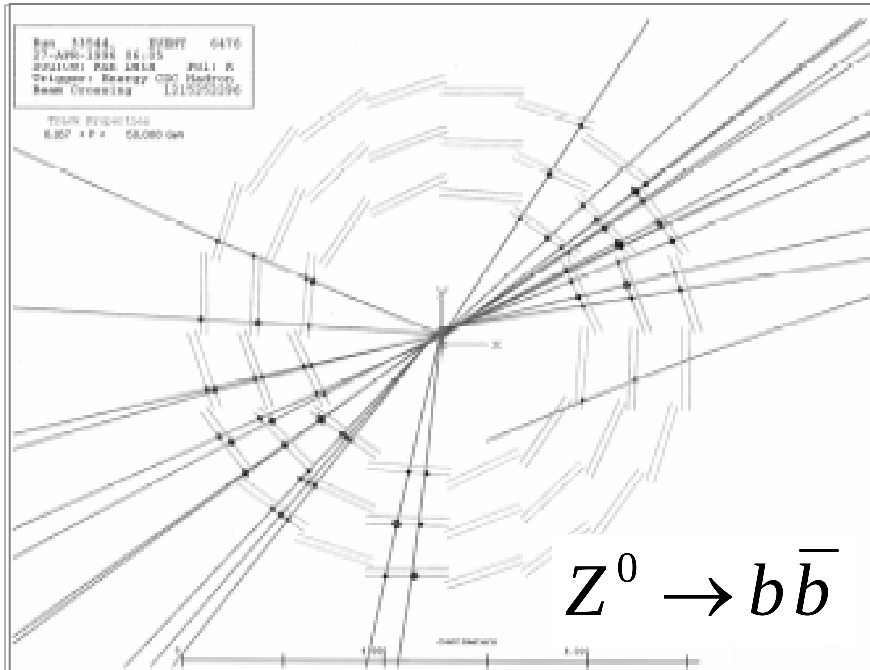

FIG. 32. End view of a detector with a reconstructed event of type $Z^0 \rightarrow b\bar{b}$.

further developments:

- fully depleted CCDs for X-ray measurements
- thinning to ~50 μm to reduce multiple scattering + sec. interactions
- read-out of every column separately with 50MHz

applications outside HEP → RR

R&D on CCDs for ILC vertex detector (LCFI-collab. – DESY PRC 26.5.05)

very ambitious:

20μm pixels
→ δx~3μm

10^9 pixels

60μm thick
"unsupported"

50μs read-out
(50 MHz!)

noise: 60e

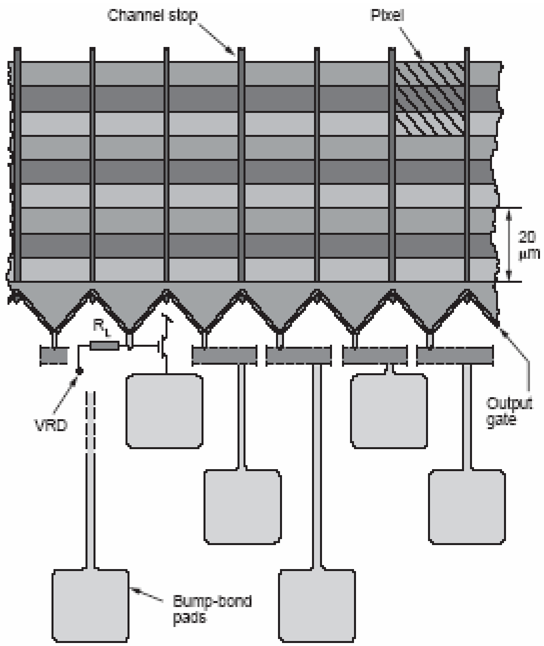

Fig. 5. Edge of CPCCD in region of interface to readout chip. For one channel, one option for the on-CCD charge sensing circuit is indicated.

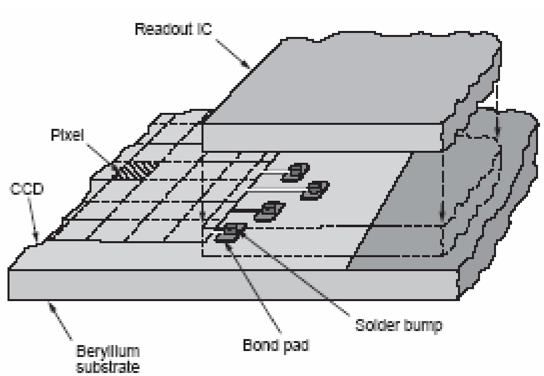

Fig. 6. Exploded isometric view of the interconnect region between CPCCD and readout chip.

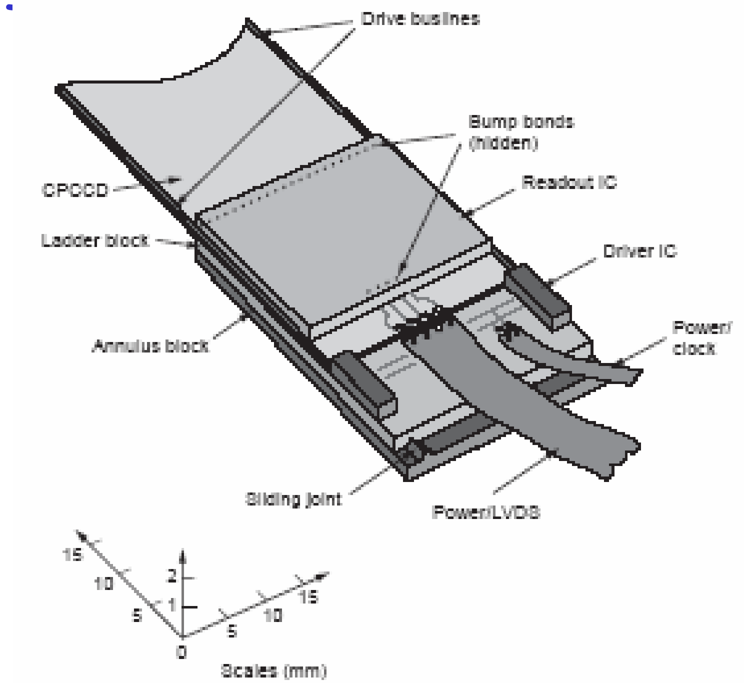

Fig. 7. Layout of components at the end of ladder. A compression spring establishes correct engagement of the sliding joint between the blocks, while a tensioning spring helps stabilise the shape of the ladder.

CPCCD1

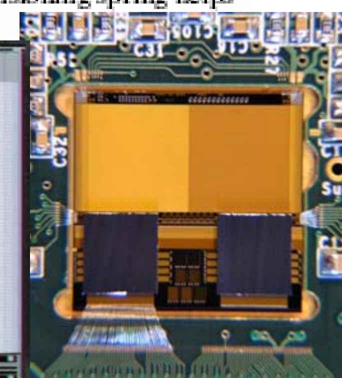

bonded module

4.5 Hybrid Pixel Detectors

Principle: separate detector-electronics

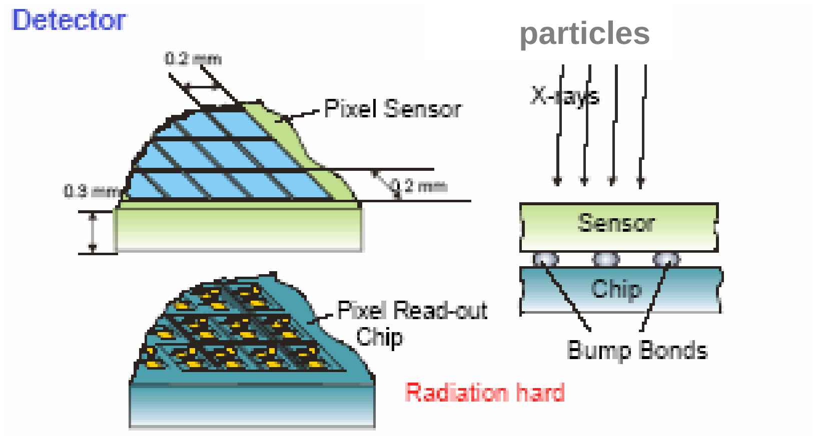

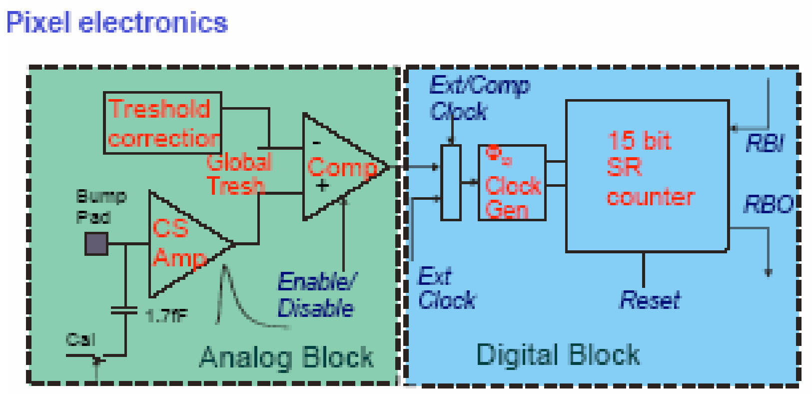

bump-bonding

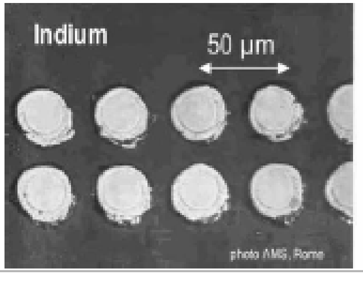

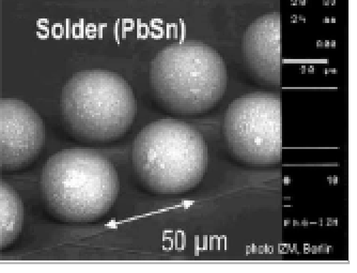

Summary Hybrid Pixel Detectors

- technology well developed, m^2s used in LHC-experiments (ALICE, ATLAS, CMS), synchrotron rad., radiology,…
- already experience in actual experi-ments
- high degree of flexibility in design → many developments in progress !
- radiation hardness achieved,
- "any" detector material possible (Si, GaAs, CdTe,…)
- typical pixel dimensions > 50 µm,
- high speed: e.g. 1 MHz/pixel,
- (effective) noise ~100e achieved
- limitations for particle physics is detector thickness, power and possibly minimum pixel size

4.6 Monolithic Pixel Detectors

Idea: radiation detector + amplifying + logic circuitry **on single Si-wafer**

- dream! 1st realisation already in 1992
- strong push from ILC → **minimum thickness, size of pixels and power !**
- so far no large scale application in research (yet)

CMOS Active Pixels

(used in commercial CMOS cameras)

Principle:

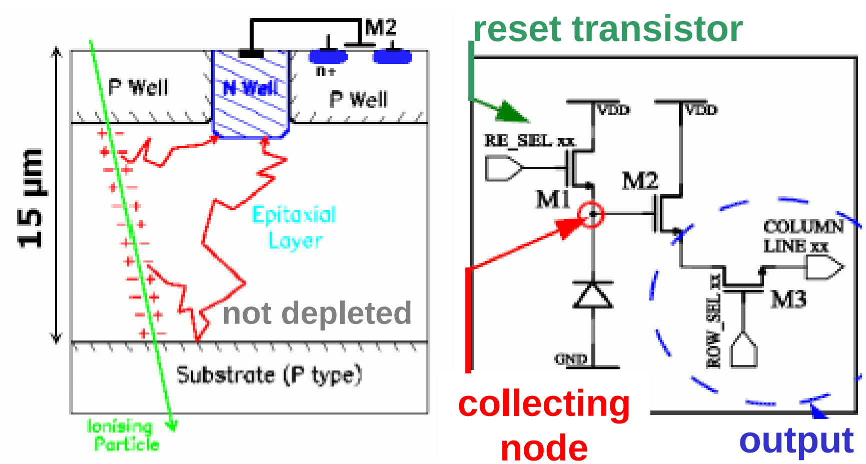

- technology in development – with many interesting results already achieved

example: MIMOSA (built by IReS-Strasbourg; tests at DESY + UNIHH)

3.5 cm^2 produced by AMS (0.6µm)
14 µm epi-layer, $(17\mu m)^2$ pixels
4 matrices of 512^2 pixels
10 MHz read-out (→ 50µs)
120 µm thick

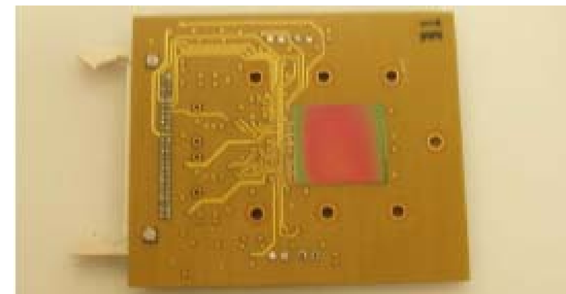
Chip mounted on PCB board

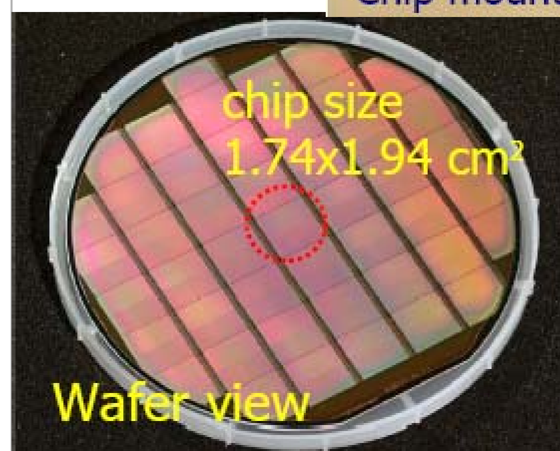

Results (source and beam tests):

- pulse height ^{55}Fe in single pixel

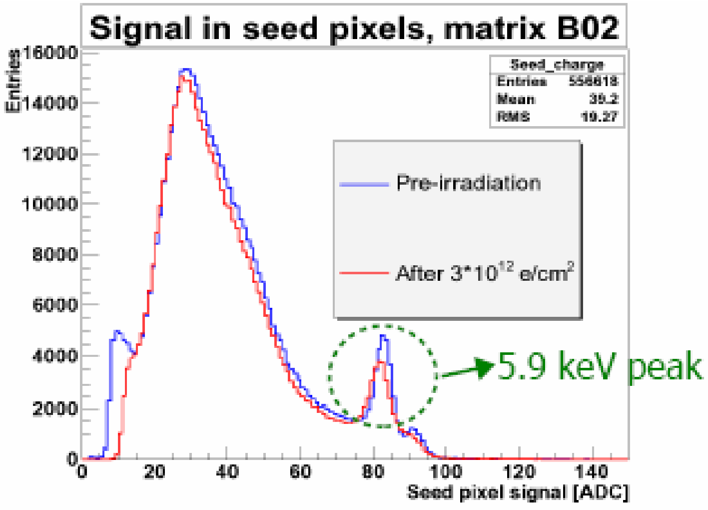

- pulse height 6 GeV electrons 9 pixels

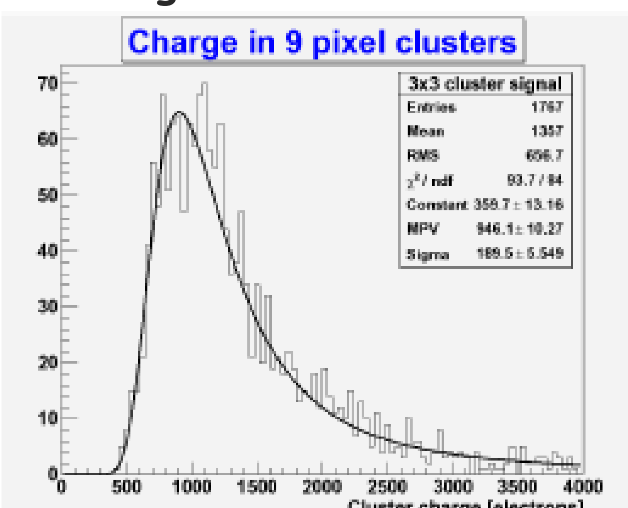

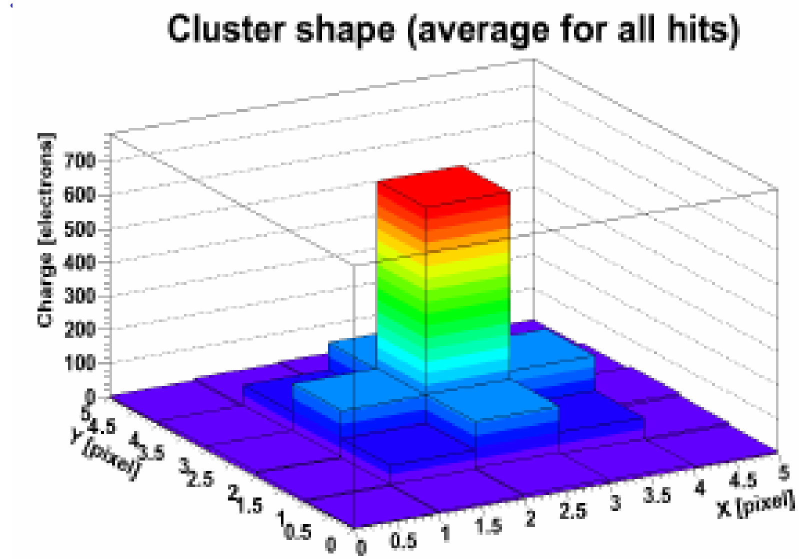

- signal ~500 e – noise 22 e
- resolution few μm (under analysis)
- charge collection < 100ns
- most of charge in 9 pixels

Summary: (work in progress)

- performance demonstrated
- small signals → pick-up sensitivity
- rad.hardness still to be demonstrated for hadrons – ok for photons (ILC)
- low cost (1€/4096 pixels) due to std. technology

develop and see !

Layout of an ILC Vertex Detector

- 5 cylindrical layers (L0 → L4)
- variable pixels 20μm(L0) - 40μm(L4)
- reduce readout t 25μs(L0) – 50μs(L1)
- <Power> 3-30W (dep. on duty cycle)

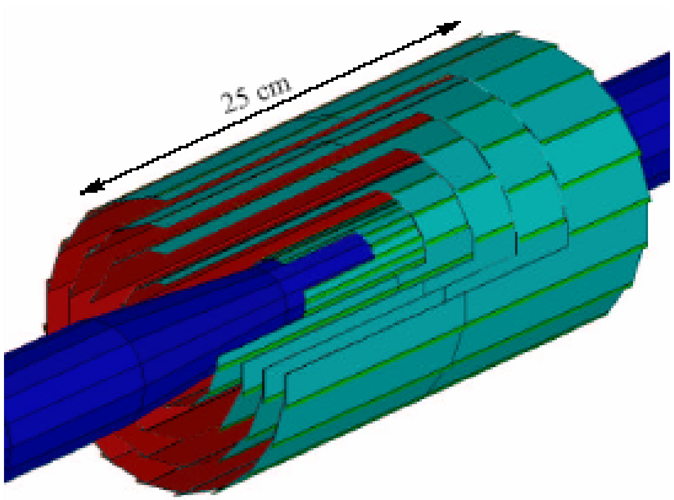

Layer	Radius (mm)	Pitch (μm)	$t_{r.o.}$ (μs)	W_{lad} (mm)	N_{lad}	N_{pix} (10^6)	P_{diss}^{inst} (W)	P_{diss}^{mean} (W)
L0	15	20	25	7	20	25	<100	<5
L1	25	25	50	15	26	65	<130	<7
L2	37	30	<200	24	24	75	<100	<5
L3	48	35	<200	24	32	70	<110	<6
L4	60	40	<200	24	40	70	<125	<6
Total					142	305	<565	<29

DEPFET Pixel Detectors

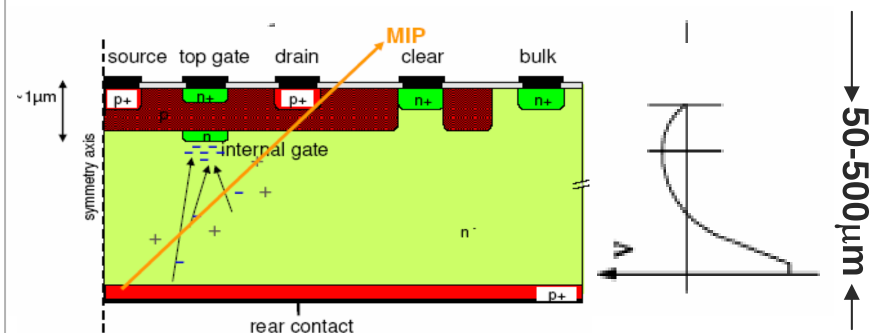

- sideward depletion (Si-drift chamber)
- potential minimum for e⁻ ~1μm underneath transistor channel by "deep" n-implant
- transistor channel steered by external gate and by internal gate
- very low C (~fF) → low noise (2e for circular structure, 10 e for linear structure)
- achieved amplifications ~400pA/e (int.gate)

"outstanding" performance → R&D for:

- vertex detectors
- X-ray astronomy
- SR-research
- biomedical applications

Matrix readout

(ILC 13x100mm² 25µm² pixels-5W):

- connect gates/clears horizontally to select/clear signal rows
- connect drains(+sources) vertically and amplify I or V → no shift of charge !!!
- sequence: enable row → read ($I_{sig}+I_{ped}$) → clear → subtract (I_{ped}) → next row

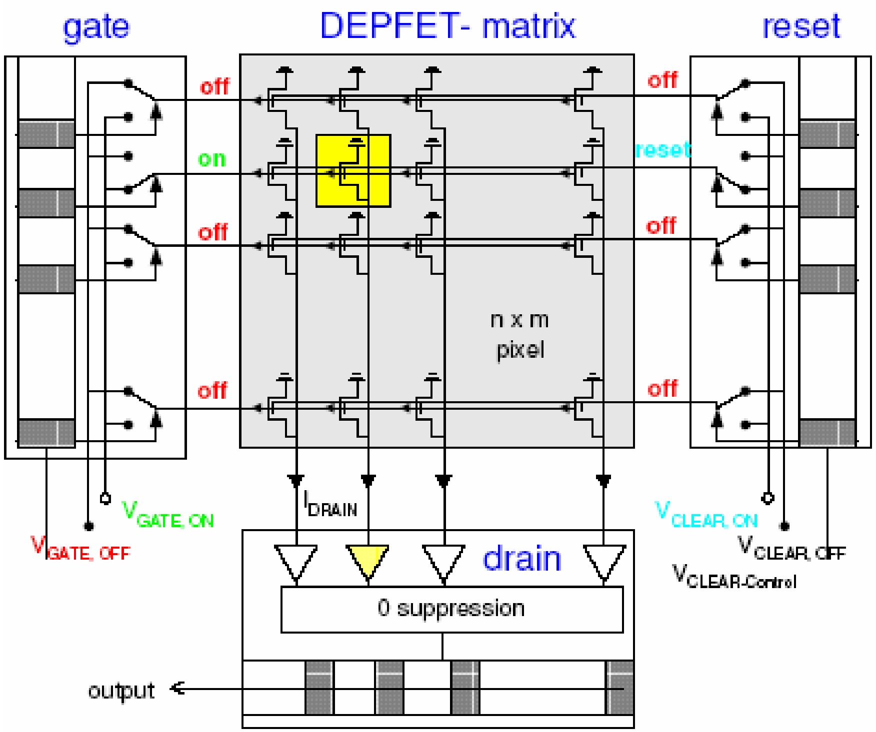

- read 10x2048 rows in 50 ns (20 MHz)

4.7 Summary

- starting with Si-strip detectors in 1980 Si-detectors became a central tool in particle physics, SR research, medical applications,… are following
- R&D driven (and most advanced) in particle physics – it still has to be demonstrated if these developments also satisfy the requirements of the new generation of X-ray sources
- if you are interested in detectors → that's the field to join !
- European (also German) groups are leading the field
- lecture gave only a small overview → see e.g. NIMA541(2005)1-466, NIMA521(2003)1-452 + many on-going conferences and workshops

Chapter 5: Limitations of Silicon Detectors

5.1 Limitations due to technology:

- **Size:** Detectors require high quality single crystals → 200 mm Ø probably limit
- **Thickness:** Limitation due to maximum voltage (field); up to O(1mm) no problem, above special care (+cost due to special manufacturing)
- **Cost:** Is clearly a significant issue – but CMS has a >200m² Si-tracking detector!
- **Number of Channels:** limitation does **not** come from detectors but from read-out power, and connection techniques → many innovative ideas

5.2 Limitations due to radiation hardness:

- appears at present most serious limitation in particle physics (at high energy hadron colliders, like the TeVatron and the LHC)
- requirements:

$O(3 \cdot 10^{15}$ n-equ./cm^2) for 10 years LHC

for SLHC (LHC-luminosity upgrade a factor x10 higher!

present day (under installation at LHC) Si-detectors do not meet requirements (exchange of pixel detectors at LHC)

Yearly dose at LHC

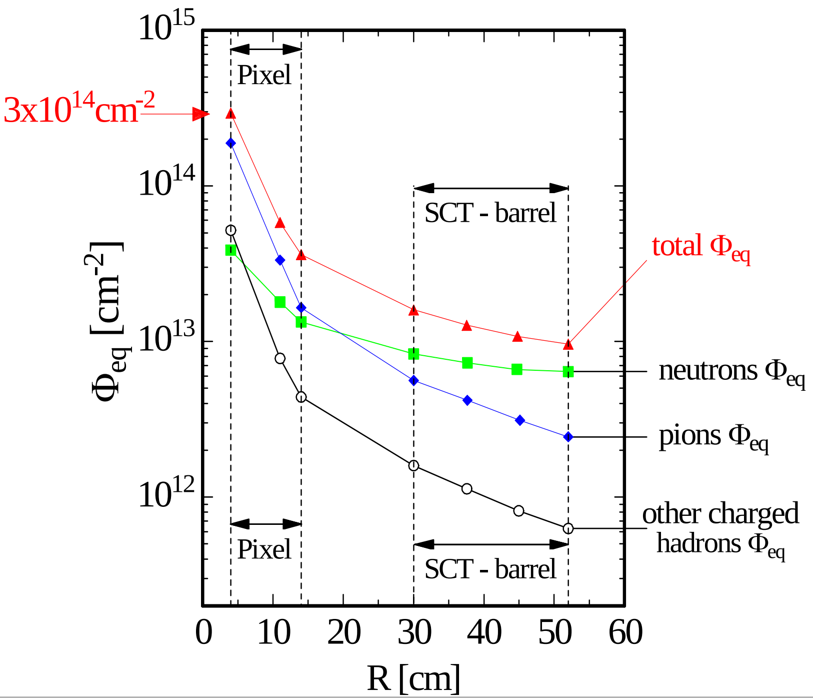

Basic Damage effects: Creation of Primary Defects

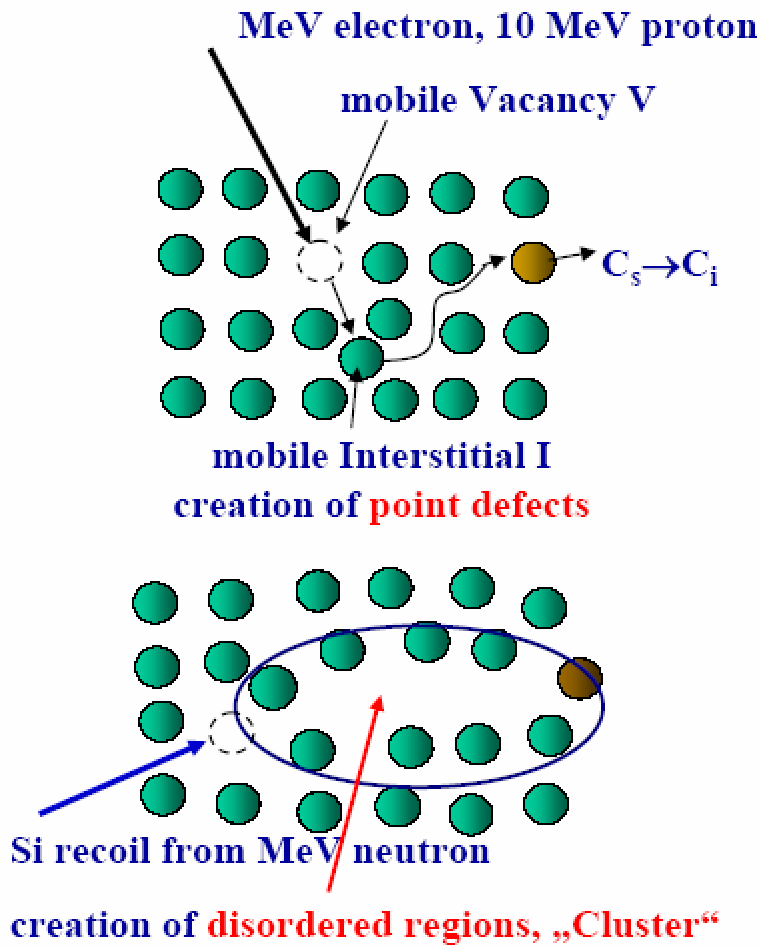

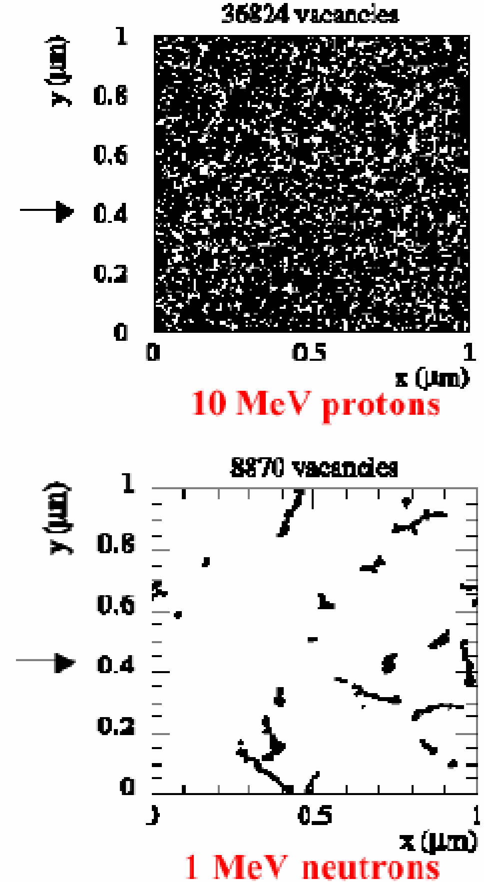

Simulation
(M. Huhtinen)

Initial distribution of vacancies in $(1\mu m)^3$ after 10^{14} particles/cm²

Gammas
electrons
low energy protons

Point Defects

1 MeV Neutrons

Cluster Damage

High energy particles

Point Defects

+ Cluster Damage

primary defects unstable → defect kinetics results in secondary defect generation

→ radiation damage a complex, multi-parameter problem

Change of macroscopic properties of Si due to radiation damage

Increase of leakage current

Introduction of defects/clusters with near to mid-gap levels as generation centers, increase of noise and power consumption, thermal run-away

$\Delta I/V = \alpha \times \Phi$

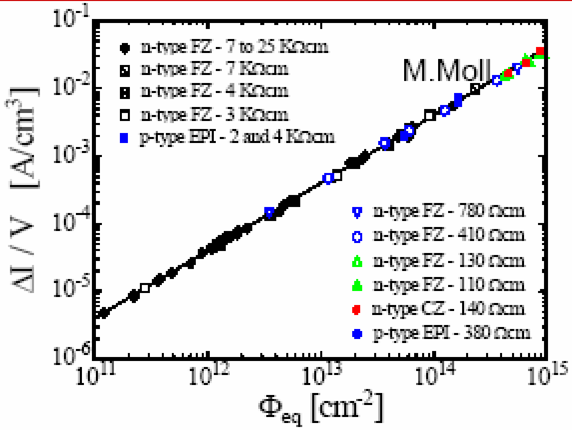

Change effective doping concentration *)

⇒ change of voltage for total depletion V_{dep}

➢ Introduction of defects which are charged in the space charge region, (acceptor creation)

➢ e.g.: V + P = VP (donor removal)

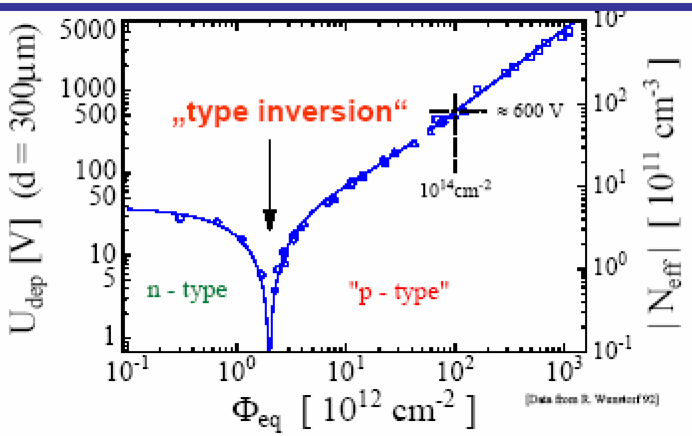

Degradation of charge collection efficiency due to increase of charge carrier trapping

$1/\tau_{eff,e,h} = \beta_{\tau\ e,h} \times \Phi$

*) at LHC the limiting effect → bias voltage > breakdown voltage of detectors (increase in leakage current reduced by T~-10°C ($I \sim \exp(-E_{Gap}/2kT)$))

How to improve radiation tolerance?

- only small fraction of defects "damaging"
  → by impurity doping try to prevent the generation of "damaging effect"

Secondary Defect Generation

Reaction schemes:

Interstitial related reactions

$I + C_s \rightarrow C_i \Rightarrow \quad C_i + C_s \rightarrow C_iC_S$

$\quad C_i + O_i \rightarrow C_iO_i$

$\quad C_i + P_s \rightarrow C_iP_S$

Vacancy related reactions

$V + V \rightarrow V_2$

$V + V_2 \rightarrow V_3$

$V + O_i \rightarrow VO_i \Rightarrow \quad V + VO_i \rightarrow V_2O_i$

$V + P_s \rightarrow VP_s$

Recombination processes

$I + V_2 \rightarrow V$

$I + VO_i \rightarrow O_i$ .....

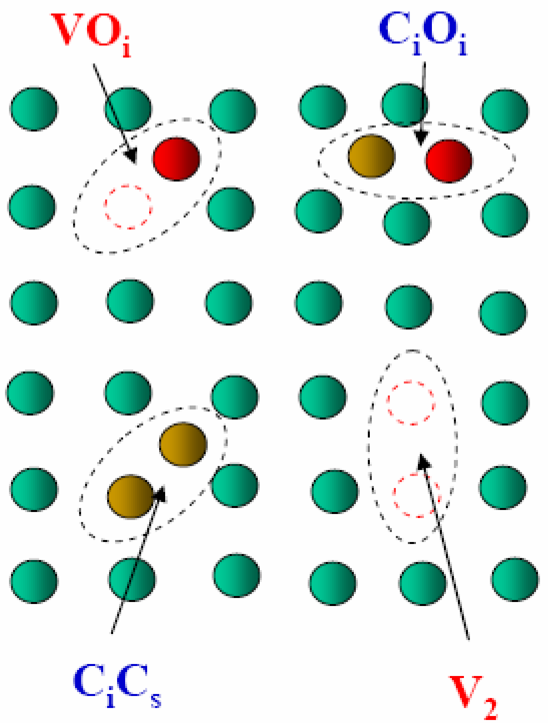

How to improve radiation tolerance?

- **Defect engineering:**
  Influence the defect kinetics by incorporation of impurities in silicon

- **Higher oxygen content $\Rightarrow$ less donor removal**

$V \nearrow$	$O \rightarrow VO$	not harmful at room temperature
$V \searrow$	$P \rightarrow VP$	donor removal

- **Higher oxygen content $\Rightarrow$ less negative space charge (V_2O-model)**

$V \nearrow$	$O \rightarrow VO$	not harmful at room temperature
$V \searrow$	$VO \rightarrow V_2O$	introduction of negative space charge

- *requires the understanding of the relation between microscopic damages and macroscopic effects*
- *detailed and complex solid state measurements*
- *precise understanding of material and production technology*
- *complicated by the fact that only small fraction of damages "harmful"*

Achievements of Defect Engineering (Univ. Hamburg et al.)

doping with oxygen has been most successful

- for point defects: (irradiation with γ's from ^{60}Co-source)
- for cluster defects insufficient improvement

Effective Doping

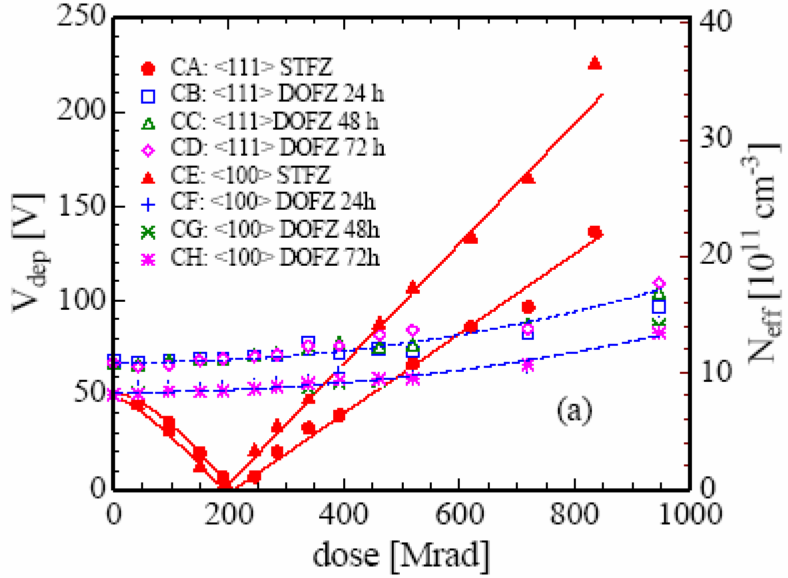

Reverse Current

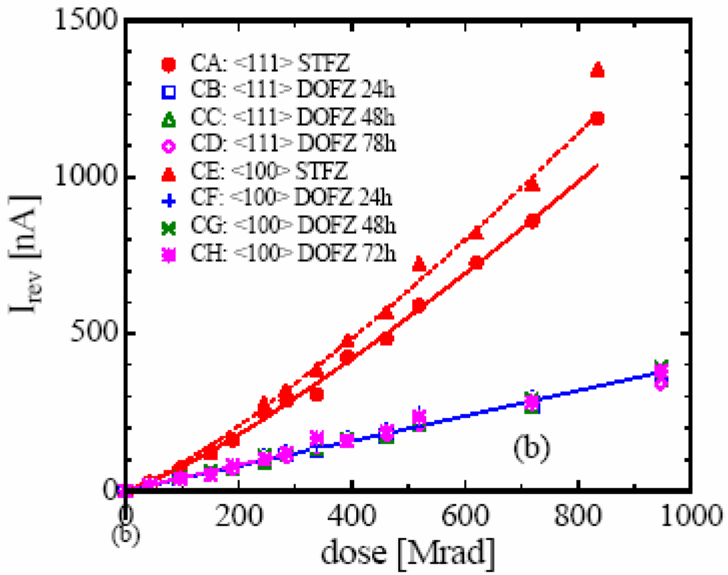

- DOFZ material: no inversion, small increase of positive space charge with dose
- Standard material: inversion at D $\approx$200 Mrad,
  V_{dep}(800 Mrad) $\approx$ 3x V_{dep}(0 Mrad)

- DOFZ material: current increase $\propto$D, at 700 Mrad I-STFZ $\approx$ 3x I-DOFZ
- Standard material: current increase $\propto D^{\gamma}$ with γ>1

Achievements of Defect Engineering (Univ. Hamburg et al.)

for point + cluster defects: (irradiation with 24 GeV/c protons)

major success for EPI-Si (50μm) on Cz-grown Si

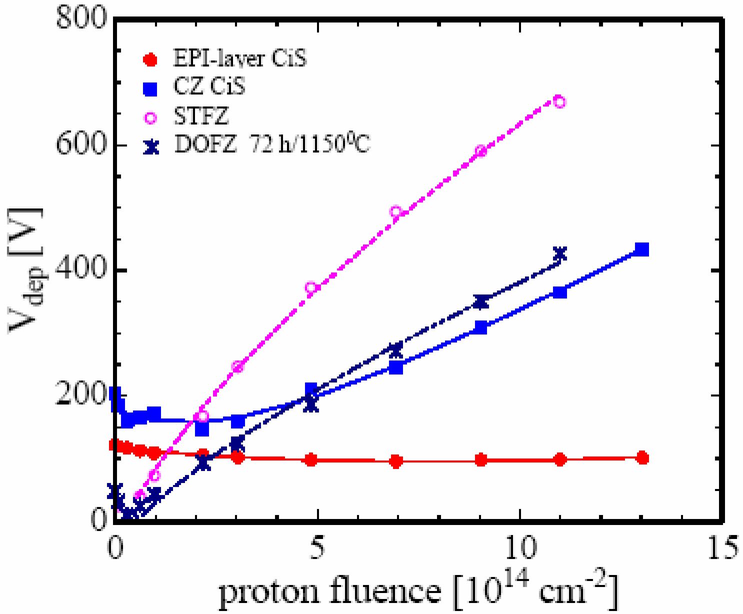

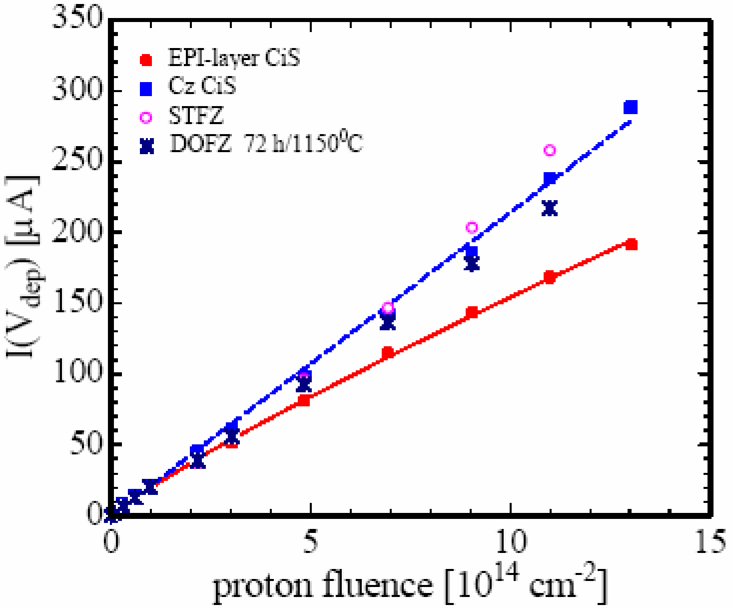

- EPI-layer (50 μm, 50 Ωcm) and Cz-silicon no type inversion
- Standard FZ-silicon (STFZ) strong increase of V_{dep} with fluence
- Oxygen enriched FZ-silicon (DOFZ, 72 h 1150°C) lower increase of V_{dep}

- Current increase of EPI-material smaller compared with all other devices (I(Vdep) normalized to 285 μm)

  Fluence dependence possibly not linear

→ radiation tolerance of material for a detector at SLHC at 4cm from beam appears to be demonstrated (but still lot's of work until realised in a detector)